UNIVERSITÀ DI PISA

Università di Pisa

FACOLTÀ DI SCIENZE MATEMATICHE, FISICHE E NATURALI

Corso di Laurea Specialistica in Fisica Applicata

Anno Accademico 2009/2010

Tesi di Laurea Specialistica

RF-knockout extraction system for the National Centre of Oncological Hadrontherapy synchrotron

Candidato:
Nicola Carmignani

Relatore:
Prof. Franco Cervelli

Correlatore:
Prof. Caterina Biscari

Contents

Introduction

The National Centre for Oncological Hadrontherapy (*CNAO*) was established on 2001 by the Italian Health Ministry. Now it is under commissioning in Pavia and will treat the first patients in one year [1].

The *CNAO* is the first Italian Centre for the treatment of patients affected by tumors by means of beams of ions: treatments with an active scanning of both protons and carbon ions will be possible.

Protons are required to have kinetic energy of about 220 MeV, while about 4.8 GeV ($400\,\frac{\mathrm{MeV}}{nucleon}$) are necessary for the $^{12}C^{6+}$ beams. A synchrotron will provide such energies.

The extraction of the beam from an hadrontherapy synchrotron must be very slow, because the extracted beam, called spill, must have low and constant intensity and must be long, in order to facilitate the measurement and control of the radiation dose delivered to patients. The duration of the extraction must be of the order of 1 s, so a multi-turn extraction (about 10^6 turns) is needed. The slow extraction is based on the third order resonance and a sextupole magnet is used to excite the resonance. The beam will be driven into the resonance by a betatron core, which accelerates the beam. The possibility of using the RF-knockout system as an alternative way to drive the beam into the resonance is also under consideration. RF-knockout method has some advantages: in particular the start and the stop of the extraction are very fast, and that characteristics is useful for some special treatment needs, such as the synchronization with the breathing of the patient.

The aim of this thesis is to verify the possibility of activate the RF-knockout extraction method and to optimize the corresponding performances with the already present hardware and minimum upgrades of *CNAO* synchrotron.

A multiparticle tracking program has been written to simulate the beam dynamics during the extraction and to optimize the parameters of the radio frequency system. Two types of signals have been studied in order to obtain a constant spill with a minimum ripple:

- a carrier wave with a frequency and amplitude modulation;

- a noise at a given range of frequencies modulated in amplitude.

The fist type of signal is commonly used in other hadrontherapy synchrotrons, as the ones in Japan and the one in Heidelberg, Germany. Nevertheless the second option results in a lower ripple of the extracted beam, as it will be shown in this thesis.

The optimized machine parameters of the two possible signals and the characteristics required for the kicker will be shown.

This work was presented at the International Particle Accelerator Conference 2010 (IPAC10) in Kyoto, Japan [2].

Chapter 1

Purpose and Project

The Radiation Therapy is one of the most important techniques of cancer treatments.

In Radiation Therapy ionizing radiation (usually X-rays or γ-rays) are used to kill the cancer cells.

X-rays are obtained by collision between an electron beam (from a linear accelerator) and a metal target. γ-rays are obtained by radioactive decays of isotopes such as ^{60}Co. X-rays are not monochromatic and the requested maximum kinetic energy ranges between 100 keV and 10 MeV, according to the depth of tumor. γ-rays are monochromatic and the available kinetic energy is of the order of 1 MeV, depending on the isotope selected.

Electron beams can also be used for Radiation Therapy. As electrons deposit all their energy in the first millimeters, they work properly to treat skin cancer. The electron beams are obtained with linear accelerators.

A new type of radiation therapy is Hadrontherapy. Hadrontherapy uses beams of hadrons, i.e. baryons, mesons or ions. The energy of the hadron beams depends on the kind of required particle and on the depth of tumor: it ranges between 100 MeV per nucleon to 500 MeV per nucleon. To have these energies for heavy particles, like carbon ions, a synchrotron is needed.

The National Centre for Oncological Hadrontherapy is the first Italian Centre for the treatment of patients affected by tumors by means of proton and carbon ions beams.

1.1 Hadrontherapy

Charged particles moving through matter interact with the electrons of atoms and deposit energy in the matter. The energy per unit of length deposited by a

charged ion in a material depends on the ion species and on its energy by the Bethe-Bloch formula [3]. The Bethe-Bloch curve, shown in fig. 1.1, describe the energy deposition. The energy per unit of length is higher when the particle energy is low.

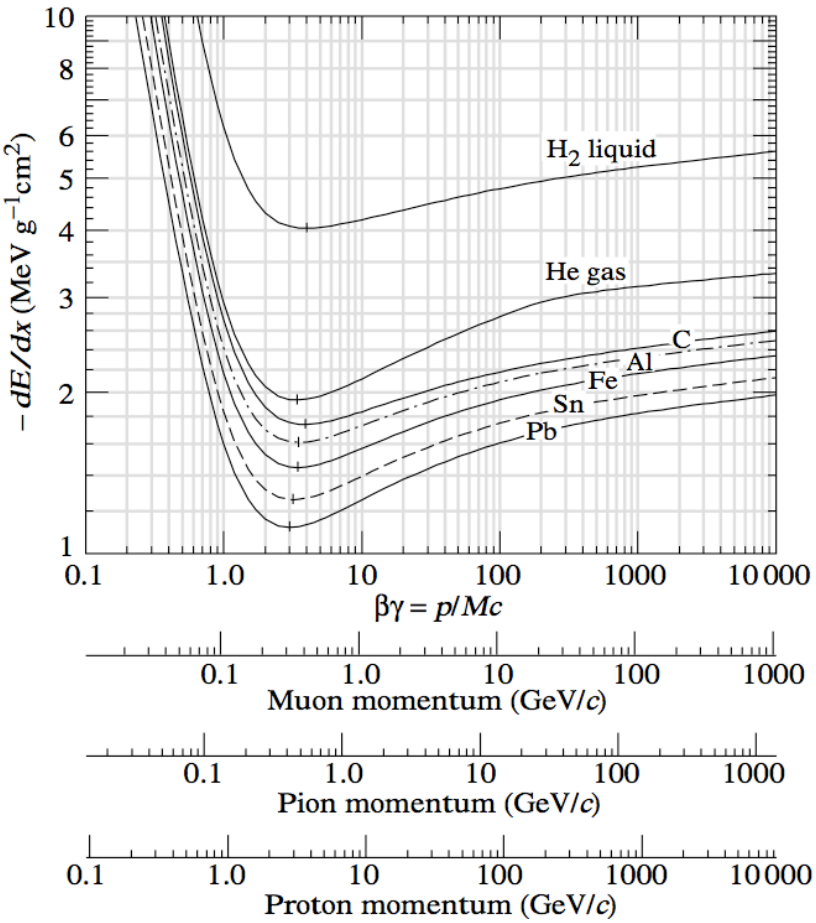

Figure 1.1: Bethe-Bloch curve. Energy deposited per unit of length by a charged particle (muon, pion or proton) in different materials.

A beam of charged ions deposits more energy per unit of length by ionization at the end of the range inside the material, i.e. when its energy is low. That phenomenon generates the so-called Bragg peak [3]. Photons and electrons have a different behavior. The energy deposited per unit of length by a beam of monochromatic photons decreases exponentially with increasing depth. Very energetic electrons lose energy due to bremsstrahlung effect, while low energetic electrons deposit all their energy in the first few millimeters of the matter.

Figure 1.2 shows the difference between the energy deposition at various depths by carbon ions and by photons of different energies: 120 keV, 1 MeV and 18 MeV.

Radiation therapy with charged particles deposits a lower radiation dose in healthy tissues surrounding the tumor so it is preferred when the tumor is located

near organs that are very sensitive to radiation.

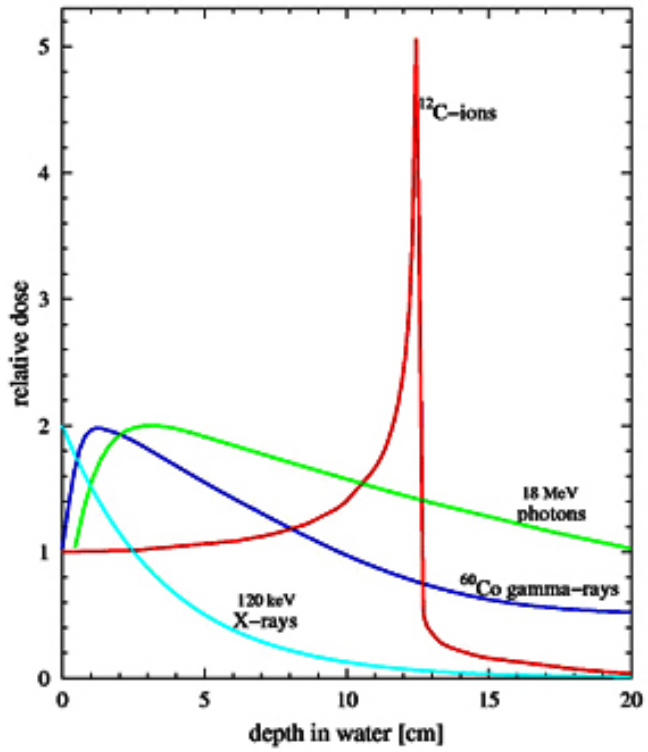

Figure 1.2: Dose deposited in water by different particles beams. The red line, which is related to the beam of $^{12}C^{6+}$, represents the Bragg peak.

The linear energy transfer (LET) is the average energy locally transfered to matter by a charged particle when crossing a distance. LET differs from the stopping power ($-\frac{dE}{dx}$): in effect LET refers to the energy deposition in a limited volume around the charged particle, while the stopping power refers to the energy lost without any volume limitation.

A high-LET radiation causes a greater biological effects, because it produces a high concentration of damaged molecules.The protons radiation has a lower LET compared to ions radiation.

There are two hadron irradiation techniques: the passive spreading and the active scanning.

The passive spreading consists on spreading the beam over a large area to treat the whole tumor. It is good for large tumors and for tumors that are difficult to immobilize. This is the most used technique.

The active scanning consists on *painting* the tumor with the beam with sub-millimeter accuracy in three dimensions. To obtain this result, some magnets near

the patient bend the beam. During the treatment, the synchrotron beam energy is changed in order to treat the tumor at different depths.

For the active scanning, well-focused beams with high spatial precision and a well defined energy are required.

CNAO will be able to treat patients with active scanning, using protons and carbon ions.

Hadrontherapy with carbon ions is conducted in Japan, at Heavy Ion Medical Accelerator in Chiba (HIMAC), since 1994. In 2009 almost 700 people have been treated with carbon ions at HIMAC and since 1994 about 5000 patients have been treated [4].

Tumors which were treated more often with carbon ions at HIMAC are:

- prostate;
- bone;
- head and neck;
- lung;
- liver;
- rectum.

Some studies have shown that mortality one year, three years and ten years after treatment is lower than mortality after other treatment options. The level of the National Cancer Institute – Common Toxicity Criteria achieved by treatment with carbon ions is less than grade 3 for almost all patients [5][6].

1.2 Characteristics of the beams at *CNAO*

The kinetic energy needed to have a Bragg peak at a depth of 26.2 cm in water is about 200 MeV for the protons and about 390.7 MeV/u for carbon ions [7].

The range of kinetic energies at the extraction is adjusted to have a penetration depth at lower energy of about 3.5 cm for both types of particles and a maximum penetration of about 27.0 cm for carbon ions and of 30.5 cm for protons. In table 1.1 the kinetic energies are summarized.

The maximum number of particles to be delivered to patients during a single spill is required to be 1.0×10^{10} for protons and 4.0×10^{8} for carbon ions. The extraction time is included between 1 s and 10 s.

particle	min energy (MeV/u)	max energy (MeV/u)	penetration at min energy (cm)	penetration at max energy (cm)
protons	60	250	3.5	30.5
carbon ions	120	400	3.5	27.0

Table 1.1: Kinetic energies of particle beams and corresponding penetration.

The extracted beam must have small transverse dimensions and a small divergence, in order to direct the beam to the tumor without deposit high dose in healthy tissues surrounding the tumor.

A quantity used in Accelerator Physics to measure the transverse dimensions of a beam and its angle is the emittance (ε_n). Dimensionally the emittance is a length times an angle and therefore the unit of measure is m $\times$ rad. The definition of emittance is given in appendix A.2.

The emittance of the extracted beam must be much smaller than the emittance of the stored beam.

Chapter 2

CNAO accelerator

The *CNAO* accelerator complex (fig. 2.1) is based on a 78 m synchrotron. The synchrotron can accelerate proton beams up to 250 MeV and carbon ion beams up to 400 MeV/u.

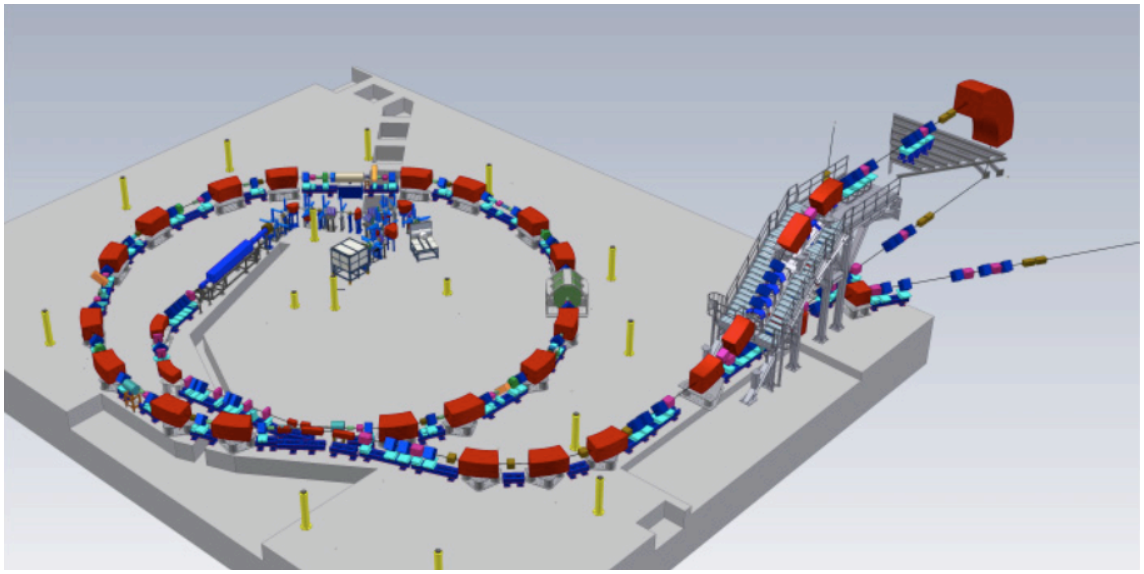

Figure 2.1: CNAO accelerator complex.

The accelerator is composed of:

- two particle sources;
- the low energy beam transfer lines (*LEBT*);
- the linear accelerator (*Linac*);
- the medium energy beam transfer line (*MEBT*)

- the synchrotron;
- the high energy beam transfer lines (*HEBT*);
- the treatment rooms;
- the experimental extraction line.

Figure 2.1 shows the accelerator complex. In the future an experimental extraction line will be added to the complex.

The sources, the *LEBT*, the *Linac* and the *MEBT* are positioned inside the synchrotron ring, the *HEBT* and the treatment rooms outside.

2.1 Injection system

The *CNAO* accelerator can use protons and carbon ions: anyway all parts of the accelerator are common for both particles.

There are two particle sources, both of them can produce protons and carbon ions. In order to keep the same charge to mass ratio in the Linac, the sources produce H_3^+ and $^{12}C^{4+}$. After the Linac all the electrons are removed.

The injection of the beam into the synchrotron is made over many turns, so the current of the sources is lower than the beam current in the synchrotron.

To have a treatment with an active scanning using the proton beam, 1.0×10^{10} particles per spill are needed. When taking into account the efficiencies of all the different components of the accelerator complex, such result is obtained if the proton sources deliver 3.20×10^{10} particles per treatment cycle.

To have a treatment with active scanning by carbon ions, 4.0×10^8 particles per spill are needed and the sources have to produce 1.49×10^9 particles per filling [8].

The beams are produced by two electron cyclotron resonance (*ECR*) ion sources. The *ECR* ion sources work frequency is 14.5 GHz [9]. The *ECR* ion sources use permanent magnets for the magnetic fields, so the total electrical power is extremely reduced. Into a volume with a low pressure gas a microwave is injected at the frequency corresponding to the electron cyclotron resonance defined by the magnetic field. The microwave heats free electrons, which collide with the atoms and cause ionization.

The *ECR* ion sources length is 600 mm, the diameter is 380 mm, the weight is 210 kg [10]. The source is shown in fig. 2.2.

Two sources can produce both H_3^+ and $^{12}C^{4+}$, after a simple switching of gases. Some others ions are also produced, as $^{12}C^{5+}$ and H_2^+: to select the required one a spectrometer is used.

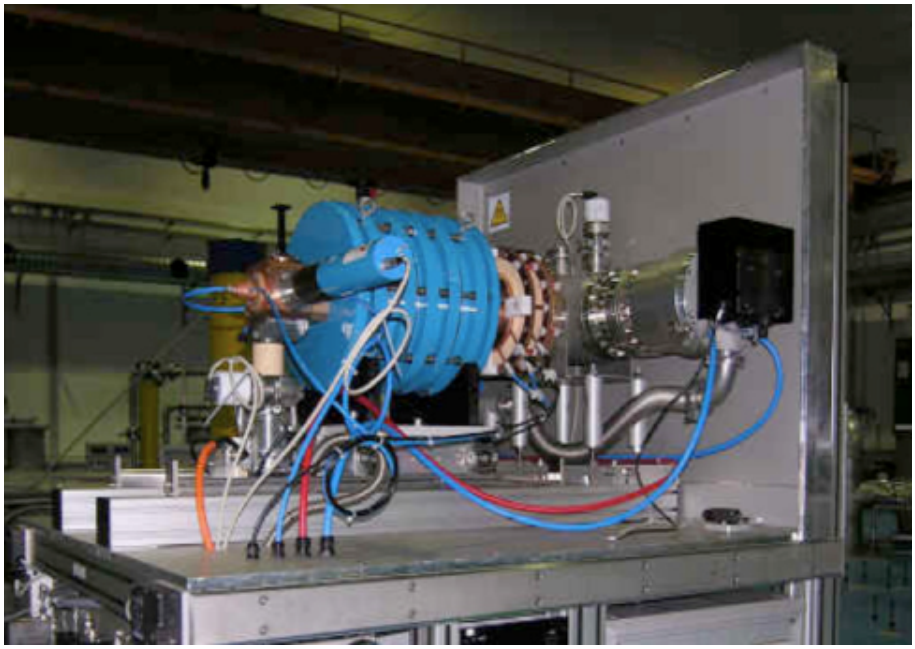

Figure 2.2: *ECR* ion source of *CNAO*.

In the low energy beam transfer line, particles kinetic energy is 8 keV for the protons and 8 keV/u for the carbon ions.

In figure 2.3 the low energy beam transfer lines are shown: magnets (dipoles and quadrupoles) and diagnostic elements can be easily identified.

At the exit of the two sources (*SO1* and *SO2*), there are two solenoids focusing the beam.

The *LEBT* is composed by three sections. The first section consists of two separate lines (*O1* and *O2*) connecting the two sources to the second section. The second and the third sections (called *L1* and *L2*) are common for both lines.

In the first sections of the *LEBT* there are the spectrometers and the quadrupole triplets for the beam focusing. The first sections end at the switching dipole.

In the second section of the *LEBT* there is a second quadrupole triplet. Between *L1* and *L2* there is a 75° bending dipole. *L2* section ends with a solenoid, positioned in front of the radio-frequency quadrupole (*RFQ*).

Inside the *RFQ* the particles have the first acceleration. The RF repetition frequency is 216.8 MHz for all ion species. The RF pulse power is $195 - 200$ kW. The kinetic energy after the *RFQ* is 400 keV for the protons and 400 keV/u for the carbon ions [11].

The 3.77 m *LINAC* accelerates the particles from 0.4 MeV/u to 7.0 MeV/u. The *LINAC* is a copy of the one of the Heidelberg Ion-beam Therapy centre (*HIT*). The resonance frequency of the *Linac* is 216.8 MHz and the RF pulse repetition freqency

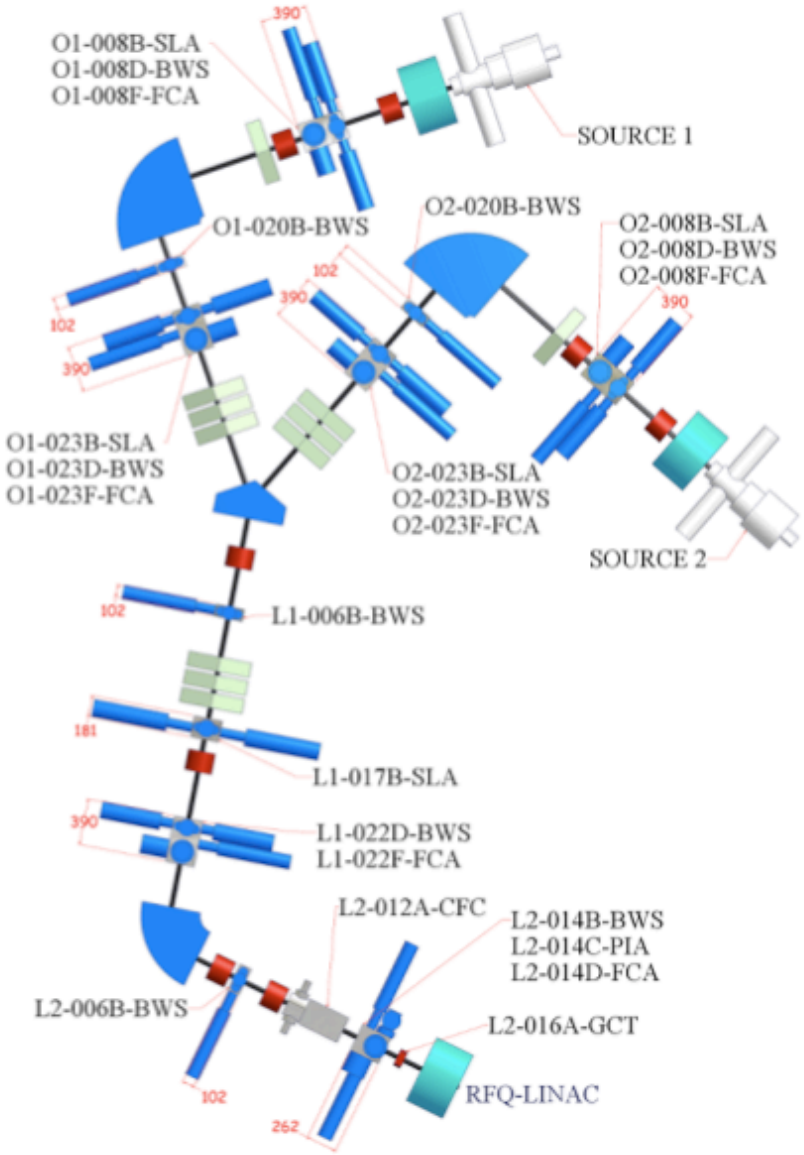

Figure 2.3: The sources and the low energy beam transfer lines.

is 10 Hz. In fig 2.4 is shown a photograph of the *LINAC* during tests at *GSI*.

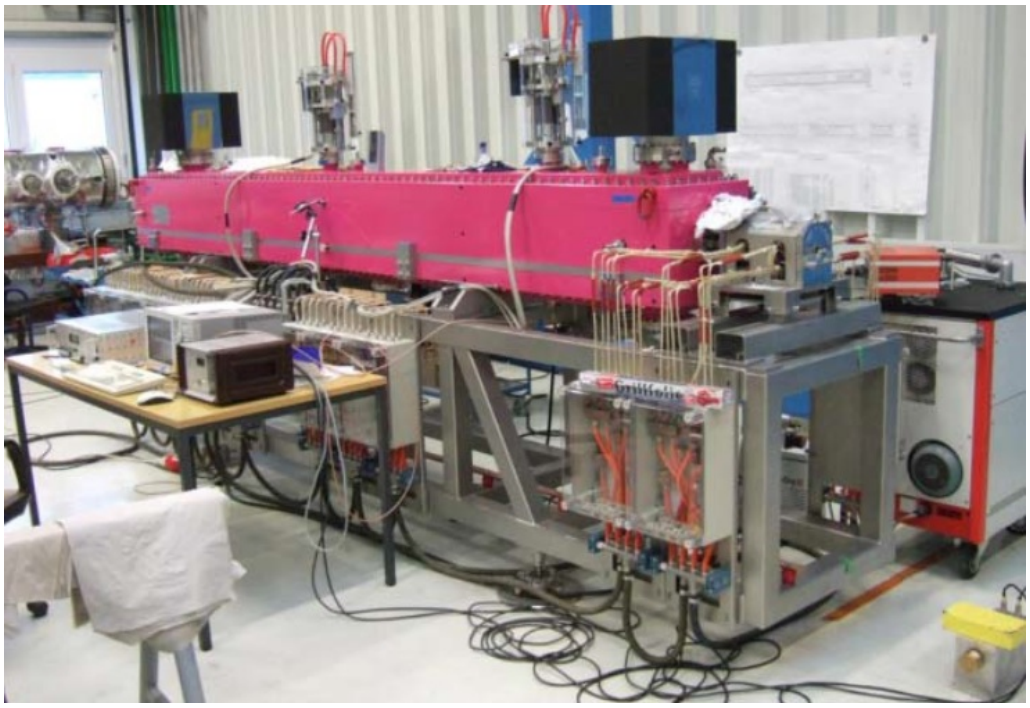

Figure 2.4: The *LINAC* under test at *GSI*.

The Medium Energy Beam Transfer line (*MEBT*) brings the proton or the $^{12}C^{6+}$ beam from the end of the *LINAC* to the electrostatic septum, where it is injected into the synchrotron. In figure 2.5 the *MEBT* line is shown.

Two dipoles divide the *MEBT* in tree segments: *M1*, *M2* and *M3*.

In the section *M1* there are four quadrupole magnets. In the section *M2* the last selection of ion species can be done with the slits, to ensure the maximum ion purity of the beam. *M3* is the section where the beam is prepared to the multi turn injection and where most of the diagnostic elements are placed [1].

Many diagnostic elements are installed along *LEBT* and *MEBT*: slits, wire scanners and Faraday cups [12].

The wire scanners can measure the beam profile: a wire crosses the beam transverse area (horizontally or vertically) and the current collected by the wire is acquired. From the contemporary information of the current and of the instantaneous position the profile of the beam is derived. Slits and wire scanners allow also to measure the beam divergence.

The Faraday cups were used to measure the beam current during the commissioning of the injection system and to monitor the current from the sources. Measurements taken with the Faraday cups are destructive.

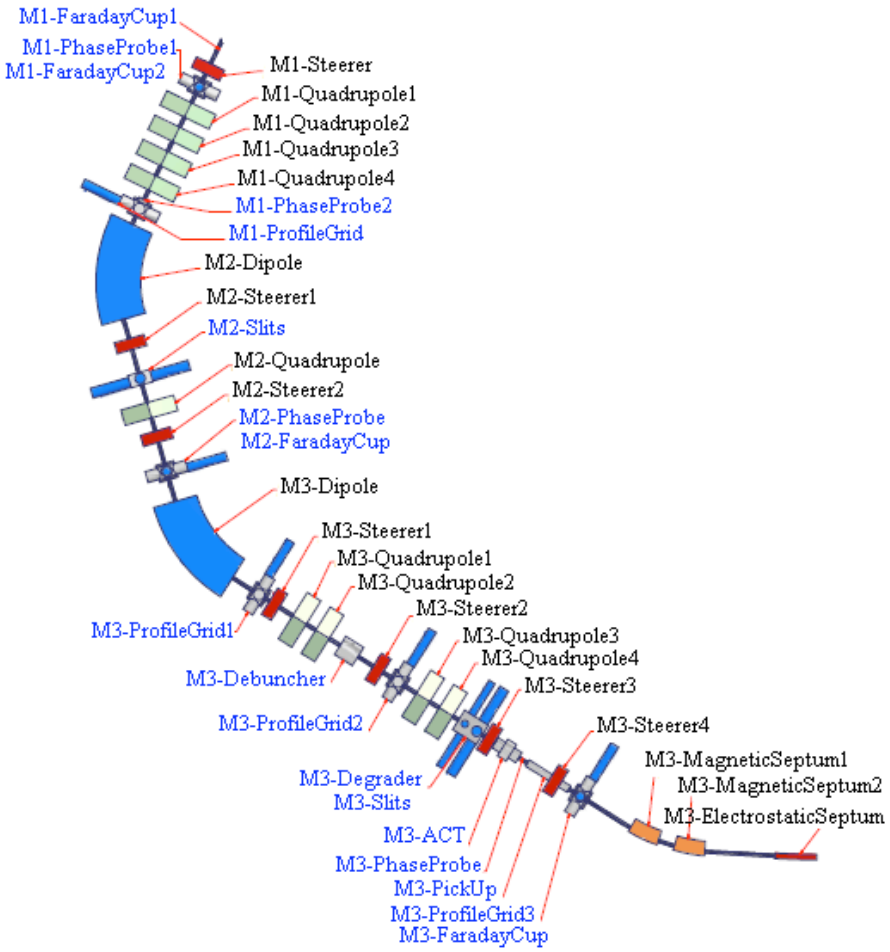

Figure 2.5: The medium energy beam transfer lines.

In order to have 1.0×10^{10} particles per extracted spill, the required current of H_3^+ ions, is 600 μA and in order to have 4.0×10^8 carbon ions per extracted spill, the required current for the $^{12}C^{4+}$ beam, is 200 μA. During commissioning of the low energy beam transfer line, currents up to 1400 μA were obtained for H_3^+ ions and up to 230 μA for $^{12}C^{4+}$ ions [13].

2.2 Synchrotron

The *CNAO* synchrotron is based of two achromatic arcs joined by two dispersion-free sections [8].

The characteristic of an achromatic beam line is that at the end of the line the position and the angle of the particle are independent of the particle energy.

In the dispersion free section the dispersion and its derivative are zero.

The lattice of the synchrotron consists of:

- 16 dipoles;
- 24 quadrupoles;
- 5 sextupoles;
- 20 correctors;
- 1 RF cavity;

In one of the two dispersion-free section there are the injection electrostatic septum and the magnetic extraction septum. In the other one there are the RF-cavity and the resonance-driving sextupole.

In figure 2.6 the geometry of the synchrotron is shown and in table 2.1 the synchrotron characteristics are summarized.

2.2.1 Main magnets characteristics

In the synchrotron there are 16 identical dipoles, each bending the beam of $\frac{\pi}{8}$ rad. These dipole magnets have a *H-type* design, are rectangular and have parallel end faces.

The main characteristics of the dipoles are shown in table 2.2.

In figure 2.7 the geometry of the dipoles is shown.

The particles curvature radius can be derived from the effective magnetic length at maximum field of the dipoles:

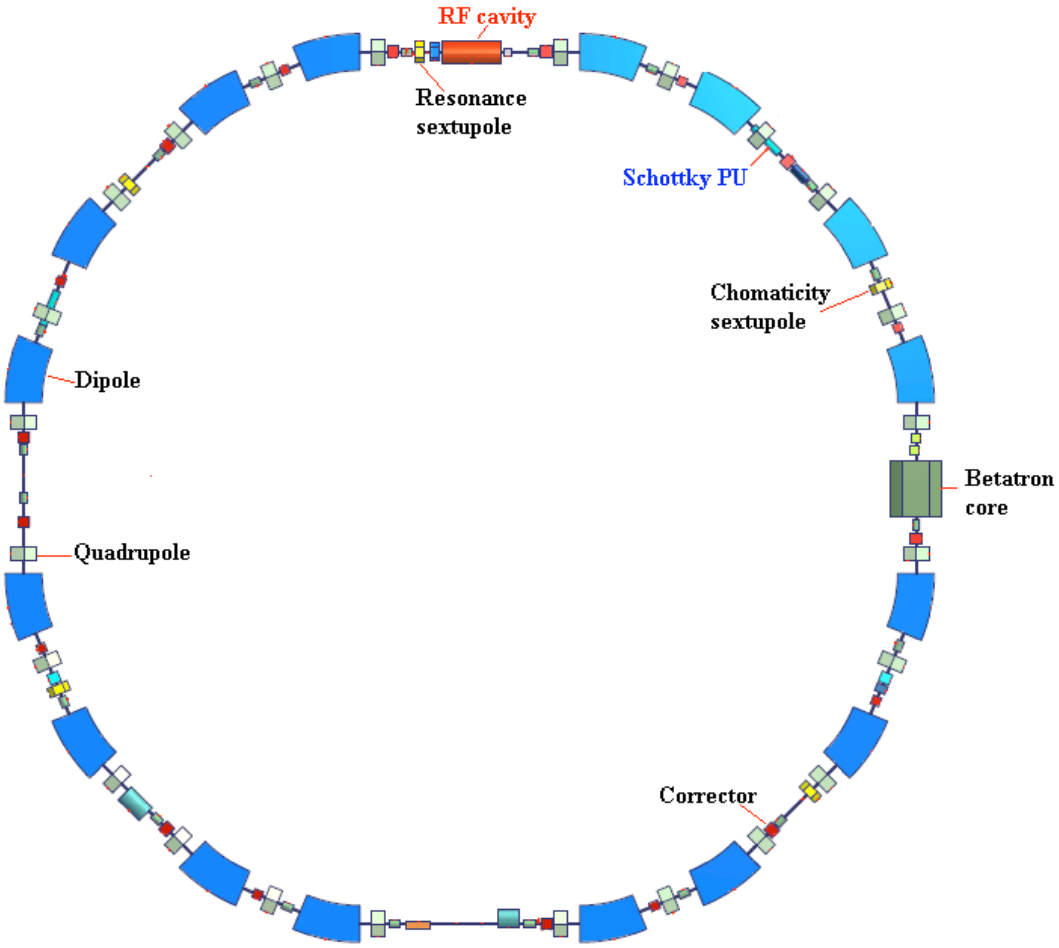

Figure 2.6: *CNAO* synchrotron.

Circumference	77.64 m
Particles	p or $^{12}C^{6+}$
Proton injection energy	7.0 MeV
Protons extraction energy	60 ÷ 250 MeV
$^{12}C^{6+}$ injection energy	7.0 MeV/u
$^{12}C^{6+}$ extraction energy	120 ÷ 400 MeV/u
Revolution frequency	0.469 ÷ 2.76 MHz
Number of dipoles	16
Number of quadrupoles	24
Number of sextupoles	5
Horizontal tune at injection	1.739
Vertical tune at injection	1.779
Horizontal tune at extraction	1.666
Vertical tune at extraction	1.720
Dipole curvature radius	4.23 m

Table 2.1: *CNAO* synchrotron characteristics.

Overall length	1.8930 m
Overall width	1.0893 m
Overall height	0.7060 m
Gap height on central orbit	0.0720 m
Weight	8 t
Nominal maximum field	1.5 T
Current for maximum field	2778 A
Effective magnetic length at max. field	1.661 m
Field quality, $\Delta B/B$	$\leq \pm 2 \times 10^{-4}$

Table 2.2: Main characteristics of the dipoles.

$$\rho = \frac{\mathcal{N}_d \times L_0}{2\pi} = \frac{16 \times 1.661\,\mathrm{m}}{2\pi} = 4.23\,\mathrm{m} \tag{2.1}$$

where $\mathcal{N}_d$ is the number of dipoles in the ring and L_0 is the effective magnetic length at maximum field.

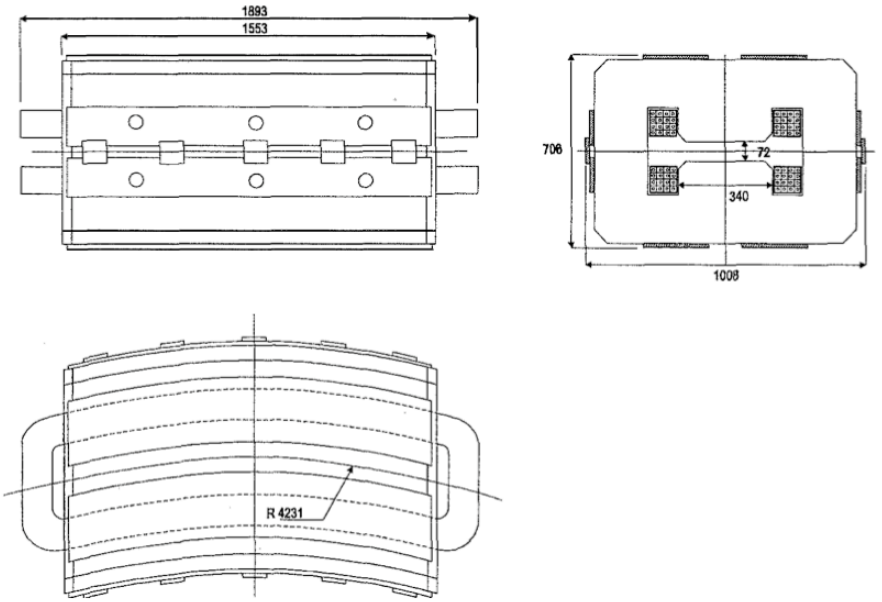

Figure 2.7: Geometry of the CNAO dipole (all dimensions in mm).

The *CNAO* synchrotron has three families of quadrupoles: two focusing and one defocusing. There are eight quadrupoles for each family [14].

The main characteristics of the quadrupoles are reported in table 2.3.

In the *CNAO* synchrotron there are five sextupoles, divided in three families. Two sextupoles families set the horizontal chromaticity and the vertical chromaticity. These four magnets are positioned in areas where the dispersion is different from zero. The fifth sextupole is placed in one of the two dispersion-free regions and drives the third integer resonant extraction [15].

Table 2.4 contains the main characteristics of the sextupoles.

The RF cavity of the *CNAO* synchrotron has a large frequency swing, between 0.4 MHz and 3.0 MHz, a very large relative permeability and a low Q factor. The

Overall length	0.4620 m
Overall width and height	0.6206 m
Aperture radius	0.0850 m
Weight	0.39 t
Nominal maximum gradient	3.65 T/m
Current for maximum gradient	540 A
Effective magnetic length at max. gradient	0.350 m
Gradient quality, $\Delta G/G$	$\leq \pm 5 \times 10^{-4}$

Table 2.3: Main characteristics of the quadrupoles.

Overall length	0.3000 m
Overall width	0.5600 m
Overall height	0.5050 m
Aperture radius	0.1000 m
Weight	0.27 t
Nominal maximum gradient	54.3 T/m^2
Current for maximum gradient	500 A
Effective magnetic length at max. gradient	0.25 m
Gradient quality, $\Delta G/G$	$\leq \pm 4 \times 10^{-3}$

Table 2.4: Main characteristics of the sextupoles.

length of the cavity is 1.5 m [16].

2.2.2 Optical characteristics of the synchrotron

An important parameter for the synchrotron is the beam magnetic rigidity. The magnetic rigidity, R, determines the effect of the magnetic field on the motion of the charged particles.

$$R = B\rho = \frac{p}{q} \tag{2.2}$$

where B is the magnetic field of dipoles, ρ is the radius of curvature of the particle, p is the particle momentum, q is the particle charge.

The beam magnetic rigidities vary by a factor of 10 from the R value of protons at the injection, to the R value at the extraction of carbon ions with maximum energy.

Table 2.5 shows the magnetic rigidities at various energies for protons and carbon ions.

Situation	kinetic energy (MeV/u)	Bρ (T m)
protons injection	20	0.65
carbon ions injection	7.0	0.76
lowest proton extraction	60	1.14
highest proton extraction	250	2.43
lowest carbon ions extraction	120	3.25
highest carbon ions extraction	400	6.35

Table 2.5: Beam magnetic rigidities (Bρ) at various energies of protons and carbon ions.

Position and Angle in the horizontal and vertical directions of the particles in an accelerator oscillate in a certain frequency range. These oscillations are called betatron oscillations and are due to the bending force of the quadrupole, which is proportional to the particle distance from the reference orbit. The reference orbit is at the quadrupoles center.

The frequency of betatron oscillations is a very important quantity in Particle Accelerator Physics: in effect, if the ratio between that frequency and the revolution frequency is a rational number, the beam is subjected to resonances.

The frequency of betatron oscillations is expressed in units of revolution frequency.

$$Q_x = \frac{f_{bx}}{f_{rev}} \tag{2.3}$$

$$Q_y = \frac{f_{by}}{f_{rev}} \tag{2.4}$$

where f_{bx} is the horizontal betatron frequency, f_{by} is the vertical betatron frequency and f_{rev} is the revolution frequency.

The tunes of the synchrotron can be changed in a large range: $1.05 < Q_x < 1.95$ and $1.05 < Q_y < 1.95$, maintaining the two dispersion-free regions. The synchrotron is designed for slow extraction on the $\frac{5}{3}$ integer resonance.

The particle tunes at injection are:

$$Q_x = 1.739 \tag{2.5}$$

$$Q_y = 1.779 \tag{2.6}$$

at extraction:

$$Q_x = 1.666 \tag{2.7}$$

$$Q_y = 1.720 \tag{2.8}$$

The above tunes refers to particles with exact reference momentum. Nevertheless, the betatron frequency depends on particle momenta.

To better understand the problem, important parameters are chromaticity and dispersion.

The variation of tunes with particle momenta is the chromaticity ξ and it is defined by:

$$\xi_x = \frac{\Delta Q_x}{\Delta p/p} \tag{2.9}$$

$$\xi_y = \frac{\Delta Q_y}{\Delta p/p} \tag{2.10}$$

The nominal horizontal and vertical chromaticity of the *CNAO* ring are:

$$\xi_x = -3.940 \tag{2.11}$$

$$\xi_y = -1.067 \tag{2.12}$$

The dispersion is a function of the longitudinal position. It is the variation of the transversal coordinate with the particle momenta. It is defined by:

$$D_x(s) = \frac{\Delta x(s)}{\mathrm{d}p/p} \tag{2.13}$$

$$D_y(s) = \frac{\Delta y(s)}{\mathrm{d}p/p} \tag{2.14}$$

The spatial derivative of the dispersion function is the variation of the particle angle with the particle momenta. It is defined by:

$$D'_x(s) = \frac{\Delta x'(s)}{\mathrm{d}p/p} \tag{2.15}$$

$$D'_y(s) = \frac{\Delta y'(s)}{\mathrm{d}p/p} \tag{2.16}$$

The Twiss β function is important parameter to know the amplitude of the betatron oscillation.

In figure 2.8 the dispersion D_x and Twiss β functions: β_x and β_y, are shown as function of the position on the ring.

A treatment cycle at *CNAO* synchrotron lasts a few seconds and the corresponding magnetic cycle is shown in figure 2.9 [17], where the current of dipole power supply is plotted as a function of time.

The dipole current is proportional to the magnetic dipole field (if the magnets are not saturated) and the magnetic field is proportional to the magnetic rigidity.

The first plateau (b) represents the injection time, the following ramp (c) corresponds to acceleration, the second plateau (d) represents the extraction time. The length of the extraction is between 1 s and 10 s, so it is longer than the acceleration time. The e, f, g and h phases permit to reduce the magnetic hysteresis effects.

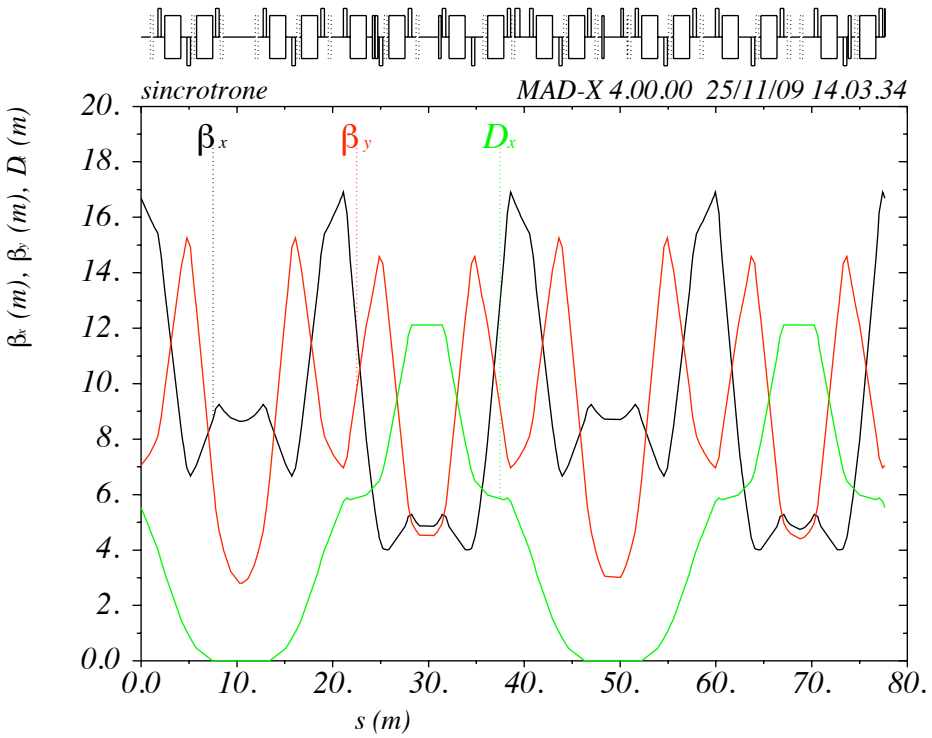

Figure 2.8: β_x, β_y and dispersion for the CNAO synchrotron.

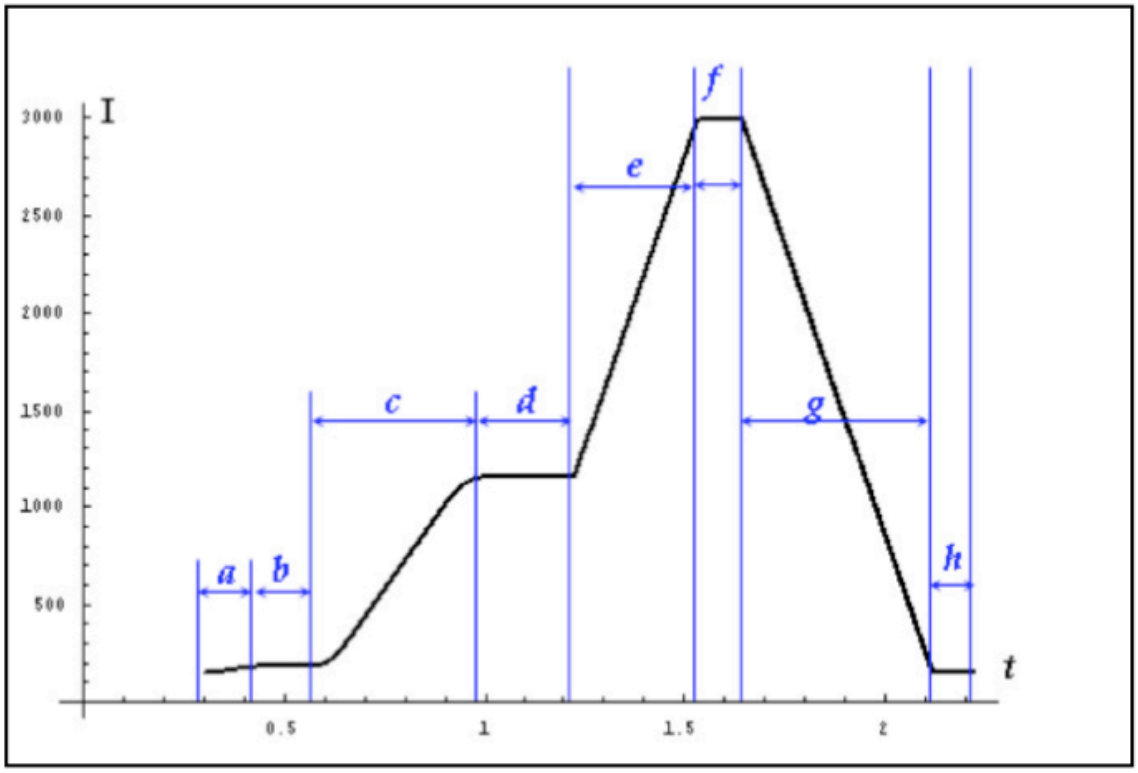

Figure 2.9: *CNAO* synchrotron magnetic cycle.

2.3 Synchrotron extraction and transport lines

The beam extraction from the synchrotron is obtained by means of an electrostatic extraction septum followed by a magnetic extraction septum after about 5 m.

The extraction is performed using the third order resonance, with the horizontal tune $Q_x = \frac{5}{3}$. The details on synchrotron extraction will be described in the next chapter.

The extracted beam is transported through the High Energy Beam Transfer Line (*HEBT*) up to three treatment rooms.

Two of them will have only an horizontal fixed beam for the treatment, the other room will have two beams: an horizontal fixed beam and a vertical fixed beam.

An upgrade of the *CNAO* complex is in project: in the second phase there will be two more treatment rooms, equipped with gantries for carbon ions [18].

Chapter 3

CNAO extraction systems

3.1 Synchrotron extraction

The beam extraction from a synchrotron can be made in one turn or in several turns. In case of hadrontherapy the extraction must be very slow. The extracted beam, called spill, must be low intensity and long, in order to facilitate the measurement and control of the radiation dose delivered to the patient.

At *CNAO* the spill duration, as written in section 1.2, ranges from 1 s to 10 s and therefore the number of turns of a complete extraction will be about $10^6 - 10^7$.

The beam extraction from a synchrotron is done with septa magnets [19], which may be electrostatic or magnetic. At *CNAO* extraction occurs through an electrostatic septum followed, at a distance of about 5 m, by a magnetic septum [20].

The electrostatic septum is an element producing an electric field that deflects the beam to be extracted, without deflecting the circulating beam. This is possible because the part of the beam to be extracted has already been separated from the circulating beam when arriving to the septum.

The magnetic septum is a special dipole which creates a magnetic field deflecting the extracted beam, without deflecting circulating beam: this is obtained thanks to the fact that the septum field is quite weak and it is almost zero in the region where there is the circulating beam.

The electrostatic extraction septum used in *CNAO* synchrotron is shown in figure 3.1.

The slow extraction for hadrontherapy synchrotrons is based on the third order resonance, excited by a sextupole magnet placed in a dispersion-free region.

There are three possible ways to drive the beam into the third order resonance:

- quadrupole driven or sextupole driven excitation;

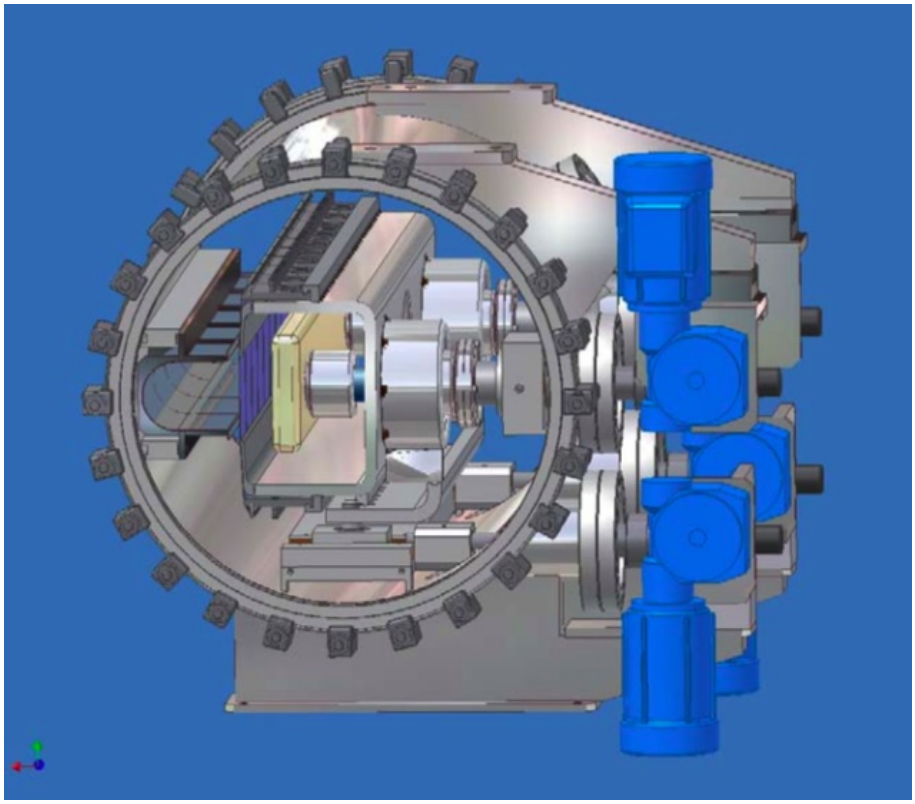

Figure 3.1: Electrostatic extraction septum.

- acceleration driven extraction;
- RF knockout extraction.

With the first method, which will not be used at *CNAO*, the value of the quadrupoles strength or the value of the resonance sextupole strength must be modified during the extraction.

At *CNAO*, the accelerator driven extraction, with the use of a betatron core, will be used as primary method and the RF knockout could be used as secondary method.

3.2 Third-order resonance

The third-order resonance occurs when the fractional part of the horizontal tune of a particle is close to $\frac{1}{3}$ or $\frac{2}{3}$.

$$Q_x = m \pm \frac{1}{3} + \delta Q \tag{3.1}$$

where Q_x is the horizontal tune value, m is an integer and $\delta Q \ll \frac{1}{3}$. δQ is called the tune distance of the particle from the resonance.

The horizontal transfer matrix of n turns of a synchrotron in normalized coordinates is:

$$M_n = \begin{pmatrix} \cos(2\pi n Q_x) & \sin(2\pi n Q_x) \\ -\sin(2\pi n Q_x) & \cos(2\pi n Q_x) \end{pmatrix} \tag{3.2}$$

where Q_x is the horizontal tune [21].

The transfer matrix for a particle close to the third-integer resonance is:

$$\bar{M}_n = \begin{pmatrix} \cos\left[2\pi n\left(m \pm \frac{1}{3} + \delta Q\right)\right] & \sin\left[2\pi n\left(m \pm \frac{1}{3} + \delta Q\right)\right] \\ -\sin\left[2\pi n\left(m \pm \frac{1}{3} + \delta Q\right)\right] & \cos\left[2\pi n\left(m \pm \frac{1}{3} + \delta Q\right)\right] \end{pmatrix} \tag{3.3}$$

The transfer matrix of three turns for a particle close to the third-integer resonance is:

$$\bar{M}_3 \simeq \begin{pmatrix} 1 & \varepsilon \\ -\varepsilon & 1 \end{pmatrix} \tag{3.4}$$

where $\varepsilon = 6\pi\delta Q$.

This means that every three turns the particle has the same starting coordinates, both in position and in angle, if $\varepsilon \to 0$, i.e. if $\delta Q \to 0$.

The simplified effect of a sextupole on the trajectory of a positively charged particle in an anticlockwise synchrotron is calculated, with the thin lens approximation, in appendix B.1. The result is shown in next equations:

$$\Delta X = 0 \tag{3.5}$$

$$\Delta X' = S\,X^2 \tag{3.6}$$

$$\Delta Y = 0 \tag{3.7}$$

$$\Delta Y' = 0 \tag{3.8}$$

where S is the *normalized sextupole strength*, defined in equation B.18. A sextupole, in first approximation, changes only the horizontal particle divergence.

Using matrix 3.3 and the simplified effect of a sextupole of equations 3.5, 3.6, 3.7 and 3.8, the change in position and divergence of a particle close to third order resonance after three turns under effect of a sextupole can be evaluated.

The result, after simplification of negligible terms, is:

$$\Delta X_3 = \varepsilon X_0' + \frac{3}{2} S X_0 X_0' \tag{3.9}$$

$$\Delta X_3' = -\varepsilon X_0 + \frac{3}{4} S \left({X_0}^2 - {X_0'}^2 \right) \tag{3.10}$$

These two equations are called the *spiral step* and the *spiral kick*.

If $S = 0$, i.e. if the sextupole is turn off, equations 3.9 and 3.10 give the same results of matrix 3.4.

3.3 Stable region

The behavior of particles in the presence of a sextupole can be better understood by studying the Hamiltonian of the system, which is called *Kobayashi Hamiltonian* [22].

After three turns, the spiral step and the spiral kick are very small quantities. The time needed for three turns in the synchrotron is very short, compared to the extraction time, so can be choose as the Unit Time.

Equations 3.9 and 3.10 can be treated as continuous functions.

Considering:

$$\frac{\mathrm{d}X}{\mathrm{d}t} = \Delta X_3 \tag{3.11}$$

and

$$\frac{\mathrm{d}X'}{\mathrm{d}t} = \Delta X_3' \tag{3.12}$$

The Hamiltonian of the system can be derived with the *Hamilton equations*. The generalized coordinate is the variable X and the generalized momentum is the divergence X'.

$$\frac{\partial \mathcal{H}}{\partial X'} = \frac{\mathrm{d}X}{\mathrm{d}t} = \varepsilon X' + \frac{3}{2} S X X' \tag{3.13}$$

$$\frac{\partial \mathcal{H}}{\partial X} = -\frac{\mathrm{d}X'}{\mathrm{d}t} = \varepsilon X - \frac{3}{4} S \left(X^2 - X'^2 \right) \tag{3.14}$$

The *Kobayashi Hamiltonian* is found by integrating equations 3.13 and 3.14.

$$\mathcal{H} = \frac{\varepsilon}{2} \left(X^2 + X'^2 \right) + \frac{S}{4} \left(3 X X'^2 - X^3 \right) \tag{3.15}$$

The Hamiltonian is a constant of the motion, because it is time independent.

For different values of $\mathcal{H}$ a particle trajectory in the normalized horizontal phase space can be found.

When the *normalized sextupole strength* (S) is zero, i.e. there is not sextupole, the trajectories in phase space (X, X') are the ones of the unperturbed particles in a linear synchrotron. Those trajectories are circles with radius $\sqrt{\frac{2\mathcal{H}}{\varepsilon}}$.

If S is not zero, the circular trajectories are distorted into *triangular trajectories*. When the excitation exceeds a certain level, the triangular trajectories become open trajectories, as shown in figure 3.2, where the stable triangular region is also identifiable.

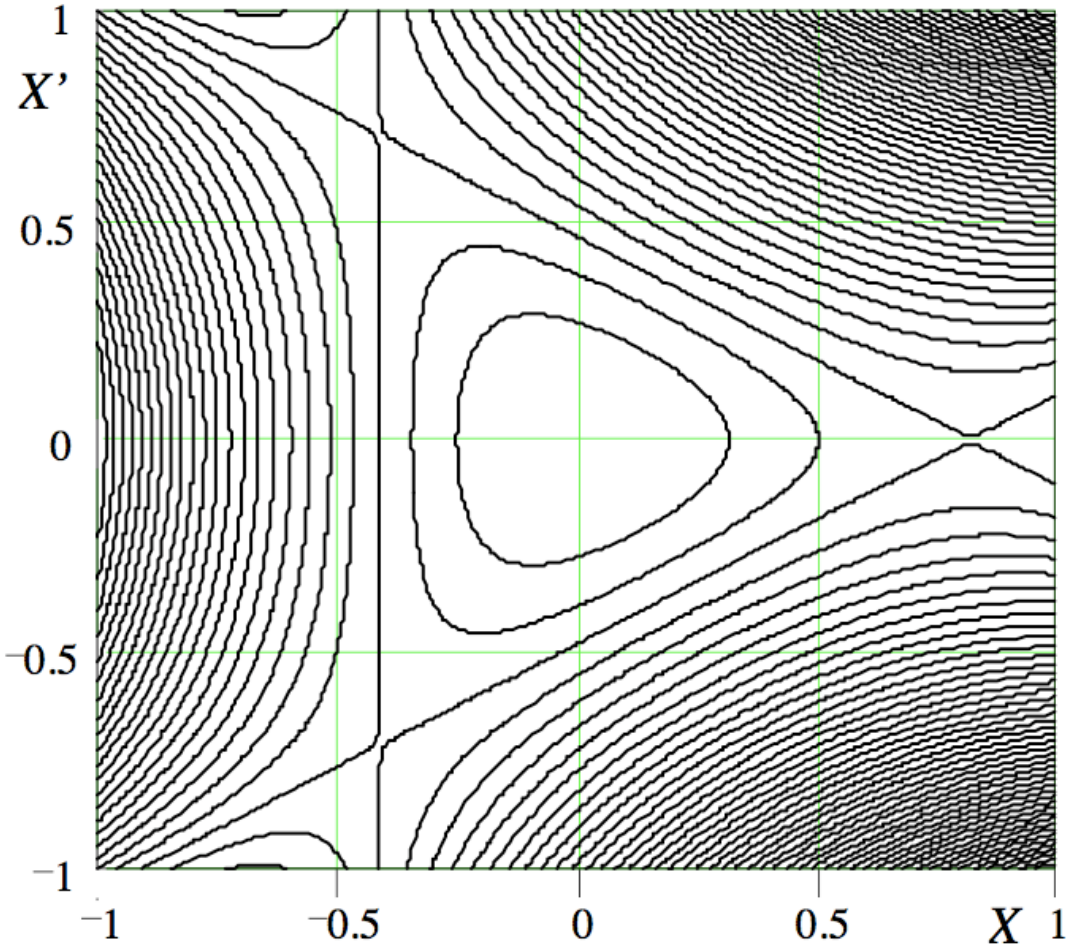

Figure 3.2: Phase-space trajectories in normalized coordinates for various excitations. These trajectories are calculated from the *Kobayashi Hamiltonian*.

The area within the triangle is called the *stable region*. If a particle is inside the triangle, its trajectory is closed; if a particle is outside the triangle, after a certain

number of turns, it will move away indefinitely.

The equations of the three straight lines at the sextupole, called *separatrices*, can be derived from the Hamiltonian. If $\mathcal{H} = \frac{8\varepsilon^3}{27S^2}$ equation 3.15 can be factorized into three pieces:

$$\left(\frac{S}{4}X + \frac{\varepsilon}{6}\right)\left(\sqrt{3}X' + X - \frac{4\varepsilon}{4S}\right)\left(\sqrt{3}X' - X + \frac{4\varepsilon}{3S}\right) = 0 \tag{3.16}$$

The tree lines are:

$$r_1 : X = -\frac{2\varepsilon}{3S} \tag{3.17}$$

$$r_2 : X' = -\frac{1}{\sqrt{3}}X + \frac{4\sqrt{3}\varepsilon}{9S} \tag{3.18}$$

$$r_3 : X' = +\frac{1}{\sqrt{3}}X - \frac{4\sqrt{3}\varepsilon}{9S} \tag{3.19}$$

The vertices of the triangle are found intersecting the three lines:

$$P_1 = \left(\frac{4\varepsilon}{3S}; 0\right) \tag{3.20}$$

$$P_2 = \left(-\frac{2\varepsilon}{3S}; -\frac{2\varepsilon}{\sqrt{3}S}\right) \tag{3.21}$$

$$P_3 = \left(-\frac{2\varepsilon}{3S}; +\frac{2\varepsilon}{\sqrt{3}S}\right) \tag{3.22}$$

The area of the stable triangle is the *acceptance* and its value is:

$$Acceptance = \frac{48\sqrt{3}\pi}{S^2}\left(\delta Q\right)^2 \pi \tag{3.23}$$

At different longitudinal positions along the ring, the stable region and the separatrices change orientation. The triangle and the three lines rotate of an angle equal of the phase advance $\Delta\mu$.

Particles with different momentum have a different stable region.

Extracted particles exit from stable region along the separatrix r_3.

To have the same extraction separatrix for different momentum, the synchrotron lattice have to satisfy the *Hardt Condition* [21]:

$$D_n \cos(\alpha - \Delta\mu) + D'_n \sin(\alpha - \Delta\mu) = -\frac{4\pi}{S}\xi_x \tag{3.24}$$

where D_n and D'_n are the normalized dispersion function and its derivative, α is the angle between the separatrix and the horizontal axis, $\Delta\mu$ is the phase advance from the resonance sextupole to the electrostatic extraction septum, S is the normalized sextupole strength, ξ_x is the horizontal chromaticity.

The horizontal chromaticity value is chosen to satisfy the *Hardt Condition*.

3.3.1 Steinbach diagram

An useful representation of the beam and of the resonance is provided by the amplitude-momentum space, called the *Steinbach diagram*, figure 3.3.

In the horizontal axis there is the momentum deviation with respect to the central orbit. This value is proportional to the tune distance, owing to the chromaticity; it is also proportional to the X particle position, owing to the dispersion. In the vertical axis there is the normalized amplitude of the ions betatron oscillation, $A = \sqrt{\frac{\epsilon}{\pi}}$, where ϵ is the single-particle emittance.

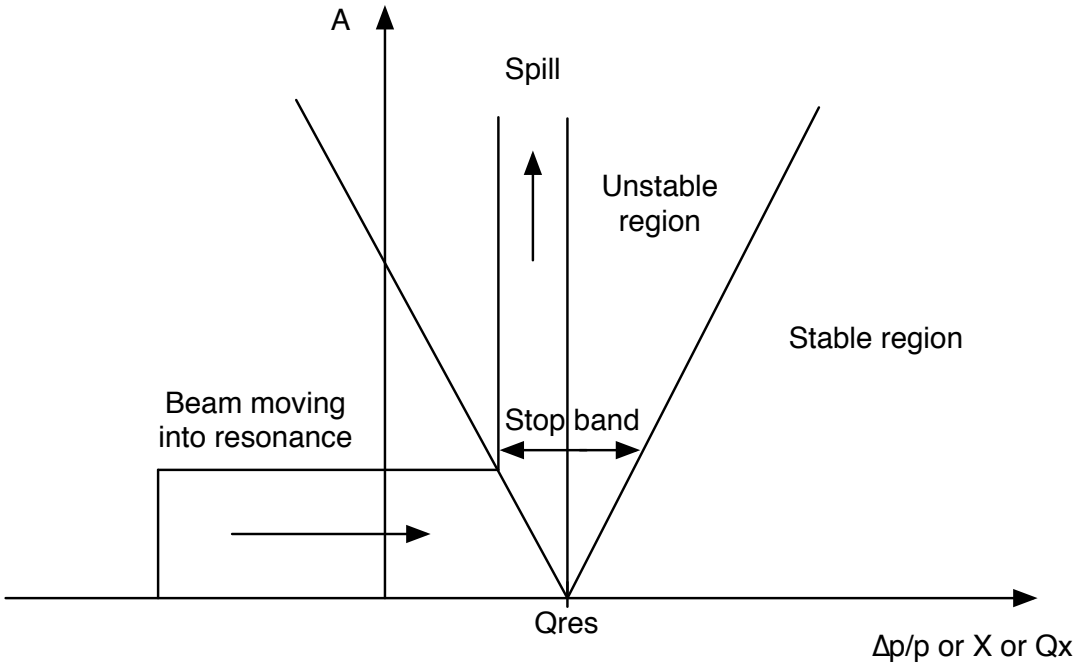

Figure 3.3: *Steinbach diagram*.

In the *Steinbach diagram* the stable region is the one outside the V region and the unstable region is inside the V.

A particle of defined momentum (i.e. with defined δQ and X position) is stable if its amplitude is smaller than the acceptance of the stable triangle defined in equation

3.23.

For a given emittance, the aperture of the V in the *Steinbach diagram* is called the *stop band* and can be derived from equation 3.23. Considering that for a stable particle:

$$\epsilon \leq \frac{48\sqrt{3}\pi}{S^2} (\delta Q)^2 \pi \tag{3.25}$$

the *stop band* is defined:

$$Q_{res} - \sqrt{\frac{1}{48\pi\sqrt{3}} \frac{\epsilon}{\pi}} |S| < Q < Q_{res} - \sqrt{\frac{1}{48\pi\sqrt{3}} \frac{\epsilon}{\pi}} |S| \tag{3.26}$$

where Q_{res} is the tune resonance value.

3.4 Betatron core extraction and RF-knockout extraction

In the magnet driven extraction the beam does not change emittance and energy. More specifically:

with *quadrupole driven extraction* the beam horizontal tune is changed, changing the quadrupole strengths, and the tune distance of the beam from the resonance decreases;

with *sextupole driven extraction* the sextupole strength is increased, so the *stop band* increases.

In *acceleration driven extraction* and *RF-knockout* the optical parameters of the synchrotron during the extraction are constant.

In *acceleration driven extraction* the beam is accelerated towards the resonance by a betatron core.

A betatron core is a circular magnetic circuit, through which the beam passes. With a coil is possible to change the magnetic flux inside the magnetic circuit. Varying the magnetic flux an electric field directed along the axis of the betatron core is induced. The electric field accelerates the beam towards the resonance [23]. In figure 3.4 a schematic view of a betatron core is shown.

In figure 3.5 the *Steinbach diagram* of the acceleration driven extraction, obtained by means of the betatron core, is shown.

The momentum spread of the beam, before the beginning of the acceleration driven extraction, must be increased until $\frac{\Delta p}{p} \simeq 0.002$. Then the betatron core accelerates the beam gradually and the beam goes in the unstable region.

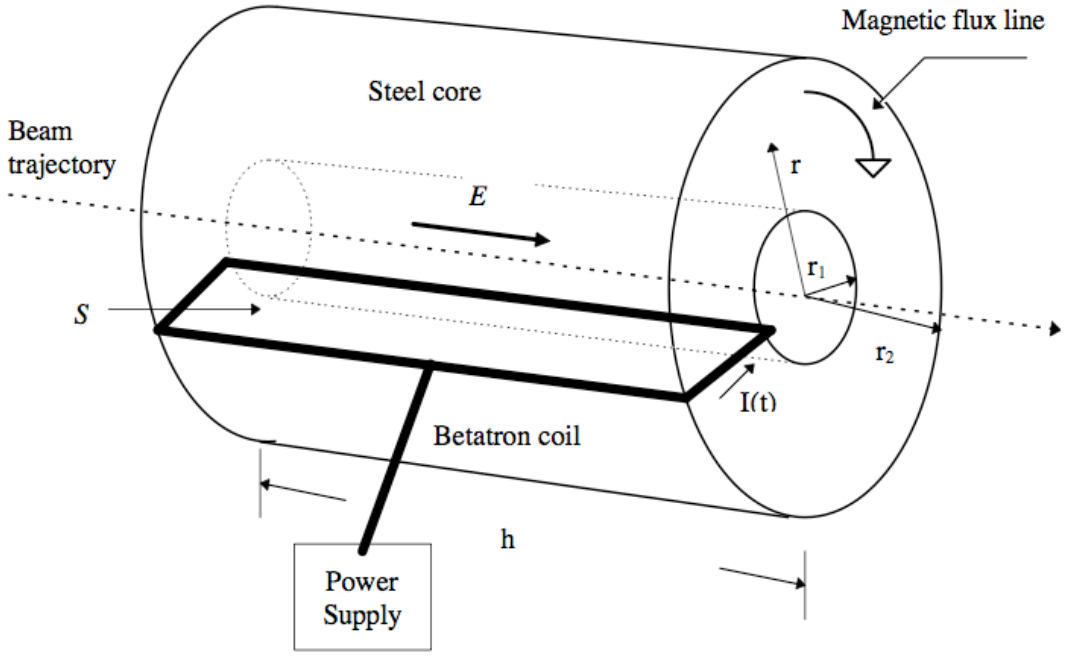

Figure 3.4: Schematic view of a betatron core.

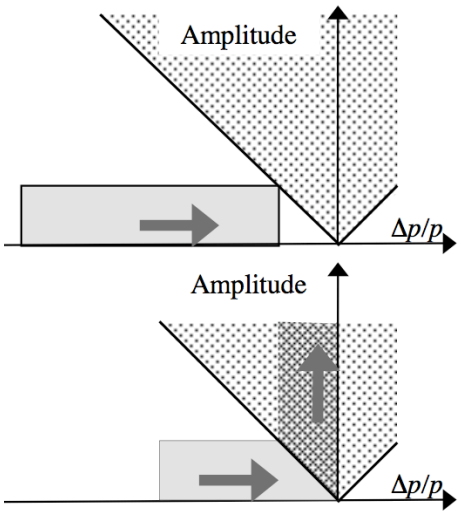

Figure 3.5: *Steinbach diagram* of the acceleration driven extraction, done with the betatron core.

With this extraction method is possible to have an extracted beam with a small $\frac{\Delta p}{p}$. The activation and deactivation of the extraction within the same synchrotron cycle is not very fast, so, to be used when the synchronization with the breathing of the patient is required, an on-off system on the extraction line must be used.

In *RF knockout extraction* the beam is excited in the horizontal phase space by a radio frequency or by a stochastic noise with the right range of frequency. The amplitude of betatron oscillation increase and, without changing the tune of the particles, they go out from the stable region.

The RF knockout extraction consists on increasing the horizontal emittance of the beam with a RF kicker. The beam will gradually leave the triangular stable region, without changing its energy. The momentum spread of the extracted beam is equal to the momentum spread of the circulating beam, unlike the case of extraction with the betatron core. To have a momentum spread as small as possible, we must keep a low momentum spread in the circulating beam.

In figure 3.6 is shown the *Steinbach diagram* of the RF knockout extraction.

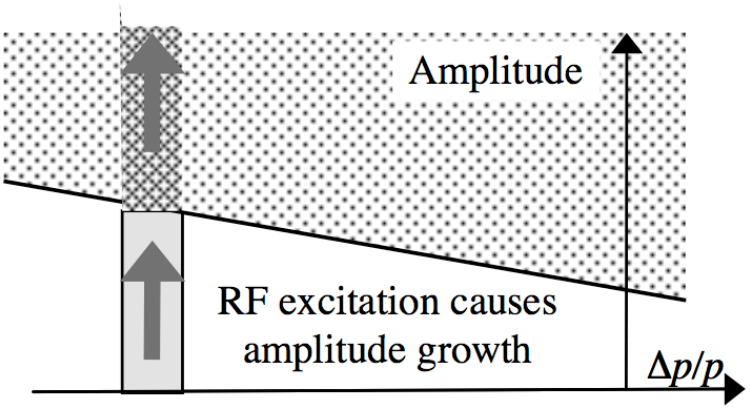

Figure 3.6: *Steinbach diagram* of the RF knockout extraction.

Chapter 4

RF-knockout

Once the beam in the synchrotron has reached the extraction kinetic energy, the resonance driving sextupole is activated to excite the resonance. The activation of the sextupole is done gradually, in few ms. The trajectories of the particles in phase space are deformed into triangles (fig. 3.2). The emittance of the beam before the activation of the resonance driving sextupole must be smaller than the acceptance defined in eq. 3.23.

The RF-knockout extraction system involves the use of a kicker, which perturbs the beam at a frequency of the order of the revolution frequency. The amplitude of the kick must be of the order of few μrad. The kicker is turned on when the sextupole is activated.

The perturbation modifies the particle divergence by a small angle. If the perturbations of each particle at every turns are similar, after many turns the beam emittance increases until it become bigger than the acceptance and some particles leave the stable region.

To have a perturbation resonant with the particle, the radio frequency must have the same frequency of the betatron oscillation, or a frequency which match the betatron oscillation.

The betatron oscillation frequency f_x is:

$$f_x = Q_x \times f_{rev} = (m + q_x) \times f_{rev} \tag{4.1}$$

where $m \in \mathbb{N}$ is the integer part of Q_x and $q_x \in \mathbb{R}$ is the fractional part of Q_x.

To match the particle oscillation, the frequency of the RF signal must be:

$$f_0 = (n \pm q_x) \times f_{rev} \tag{4.2}$$

where $n \in \mathbb{N}$.

If the horizontal chromaticity is 0, the RF frequency is determined by eq. 4.2, because the betatron oscillation frequency is determined. Therefore the signal of the kicker can be a sinusoid with frequency f_0:

$$k(t) = k_0 \times \cos(2\pi f_0 t) \tag{4.3}$$

If the horizontal chromaticity of the synchrotron is different from 0, the momentum spread produces a tune spread. Therefore the betatron frequency of each particle depends on the particle momentum.

The tune spread, ΔQ_x, can be derived:

$$\Delta Q_x = |\xi_x| \times \frac{\Delta p}{p} \times Q_x \tag{4.4}$$

where Q_x is the horizontal tune, ξ_x is the horizontal chromaticity, p is the reference momentum and Δp is the momentum spread.

If the mean momentum of the particles is different from the reference momentum, i.e. there is a momentum translation, also the tune is translated.

The tune translation δQ_x is:

$$\delta Q_x = \xi_x \times \frac{\delta p}{p} \times Q_x \tag{4.5}$$

where δp is the momentum deviation from the reference one.

If the particles of the beam have a large range of tunes, a constant frequency will not match with all particle tunes and only a small fraction of the particles are extracted with RF-knockout.

At *CNAO* synchrotron the horizontal chromaticity times the horizontal tune is $\xi_x Q_x = -3.940$, the particles have a momentum spread $\Delta p/p \simeq 0.001$ and the horizontal tune of the reference particle at extraction is $Q_x = 1.666$. The tune spread is:

$$\Delta Q_x = 3.940 \times 0.001 \simeq 0.004 \tag{4.6}$$

In the *CNAO* synchrotron, in the region of the electrostatic extraction septum, the dispersion is not 0. Therefore a momentum deviation determines also horizontal position deviation.

To improve the extraction efficiency, the distance between the circulating beam and the electrostatic extraction septum is increased by decreasing the average momentum.

$$\frac{\delta p}{p} \simeq -0.0015 \tag{4.7}$$

where δp is the mean momentum deviation from the reference one.

The momentum deviation causes an other advantage: the mean tune value changes and the stable region becomes larger.

The mean horizontal tune is:

$$\bar{Q_x} = Q_x + \delta Q_x = Q_x + \xi_x \times \frac{\delta p}{p} \times Q_x = 1.666 + 3.940 \times 0.0015 \simeq 1.672 \tag{4.8}$$

Two solutions can be applied for the RF-knockout method where the chromaticity is different from 0. The first one is the use of a signal modulated in frequency, in order to cover all the tunes range [24]. The second one is the use of a white noise in the range of frequencies suitable to cover all the tunes [25].

4.1 Frequency modulation

The first solution, with the frequency modulation, is used in many hadrontherapy synchrotrons, as the one in Chiba, Japan (HIMAC [24]) and the one in Heidelberg, Germany [26].

The signal of the kicker must be modulated by a signal $\phi(t)$ as shown in next equation:

$$k(t) = k_0 \times \cos(\omega_0 t + \phi(t)) \tag{4.9}$$

where $\omega_0 = 2\pi f_0$ is the angular frequency of the carrier wave and $\phi(t)$ is the modulating signal.

The instantaneous phase $\psi(t)$ and the instantaneous frequency $f(t)$ are defined as [27]:

$$\psi(t) = \omega_0 t + \phi(t) \tag{4.10}$$

$$f(t) = \frac{1}{2\pi}\frac{\mathrm{d}\psi(t)}{\mathrm{d}t} = f_0 + \frac{1}{2\pi}\frac{\mathrm{d}\phi(t)}{\mathrm{d}t} \tag{4.11}$$

The instantaneous frequency must match all the frequency spread of the betatron oscillation. An instantaneous frequency, varying as a saw-tooth signal centered in the frequency f_0 and with peak to peak amplitude greater than the frequency spread of the betatron oscillation, ensures this matching in a simple way. The repetition frequency of the FM signal must be much less than the betatron oscillation frequency. The betatron oscillation frequency depends on the velocity of the particles in the synchrotron and therefore on the extraction energy and on the type of particle. The

betatron frequency is of the order of 1 MHz, so the FM signal frequency can be of the order of 1 kHz.

The instantaneous frequency can be written:

$$f(t) = f_0 + G(t) \tag{4.12}$$

where $G(t) = \frac{1}{2\pi}\frac{\mathrm{d}\phi(t)}{\mathrm{d}t}$.

$G(t)$ is the modulating signal and it can be a saw-tooth signal centered in 0, with amplitude greater than the frequency spread of the betatron oscillation.

$$G(t) = \Delta f \times \left(\frac{t}{TFM} - \left[\frac{t}{TFM}\right] - \frac{1}{2}\right) \tag{4.13}$$

where TFM is the period of the frequency modulation and $\left[\frac{t}{TFM}\right]$ is the integer part of $\frac{t}{TFM}$.

An example of the function $G(t)$ is shown in figure 4.1.

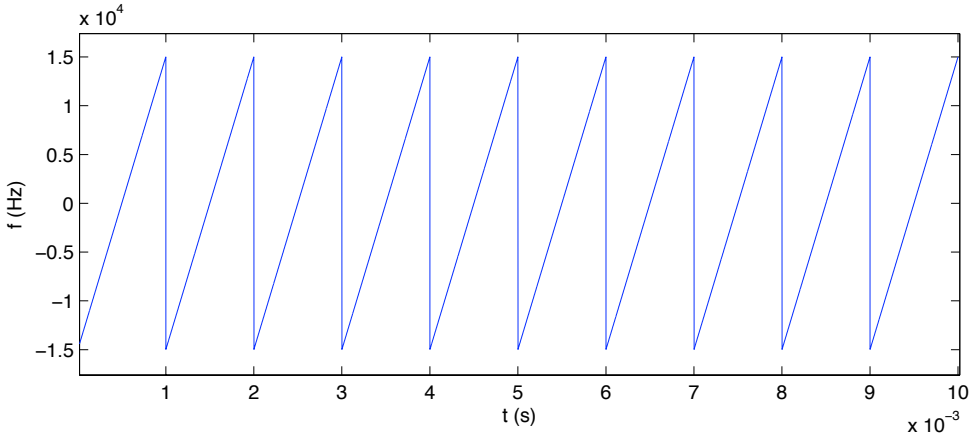

Figure 4.1: Frequency modulation signal. The period of the modulation is 1 ms and the peak to peak amplitude is 30 kHz.

The signal of the kicker $k(t)$ (eq. 4.9) can be obtained, because

$$G(t) = \frac{1}{2\pi}\frac{\mathrm{d}\phi(t)}{\mathrm{d}t} \tag{4.14}$$

therefore

$$\phi(t) = 2\pi \int_0^t G(\tau)\mathrm{d}\tau \tag{4.15}$$

Below the function $\phi(t)$ when $t < TFM$ (eq. 4.16) and the function $\phi(t)$ for all values of t (eq. 4.17) are written.

$$\phi(t) = 2\pi\Delta f \left(\frac{t^2}{2TFM} - \frac{1}{2}t \right) \quad \text{if } 0 < t < TFM \tag{4.16}$$

$$\phi(t) = 2\pi\Delta f \left(\frac{\left(t - \left[\frac{t}{TFM}\right] TFM\right)^2}{2TFM} - \frac{1}{2}\left(t - \left[\frac{t}{TFM}\right] TFM\right)\right) \quad \forall t \in \mathbb{R} \tag{4.17}$$

The signal $\phi(t)$ of eq. 4.17 is the integral of the signal of figure 4.1 and it is shown in fig. 4.2.

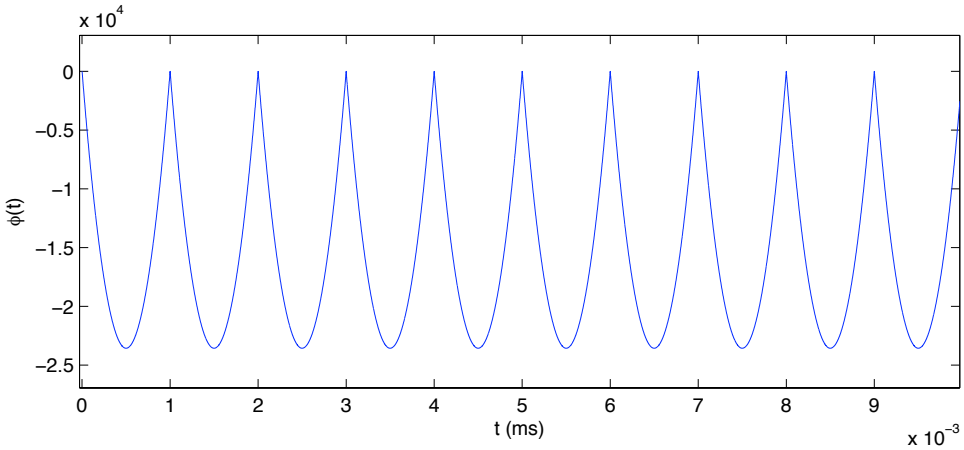

Figure 4.2: Function $\phi(t)$. It is the integral of the $G(t)$ function.

Using a kick with the signal described in eq. 4.9 all the frequencies of the particles are excited and all the beam can be extracted.

An example of a signal modulated in frequency with a saw-tooth function is shown in figure 4.3.

The carrier wave frequency is 7.0 kHz, the repetition period of the modulating signal is 1.1 ms, the peak to peak amplitude of the modulating signal is 6.5 kHz.

Those values are very different from the ones to be used in the kicker for the RF-knockout extraction. The repetition period of the modulating signal must be greater than the period of the carrier wave by about a factor 10^3, because every particle must receive a perturbation for many turns to be extracted.

If the amplitude of the frequency modulating signal is larger than the tunes spread of the particles, the kicker perturbs some particles only in the centre of the period, when the instantaneous frequency matches the betatron frequency of some particles. The result is that the extracted beam, called spill, has a ripple at frequency of the FM signal repetition, about 1 kHz.

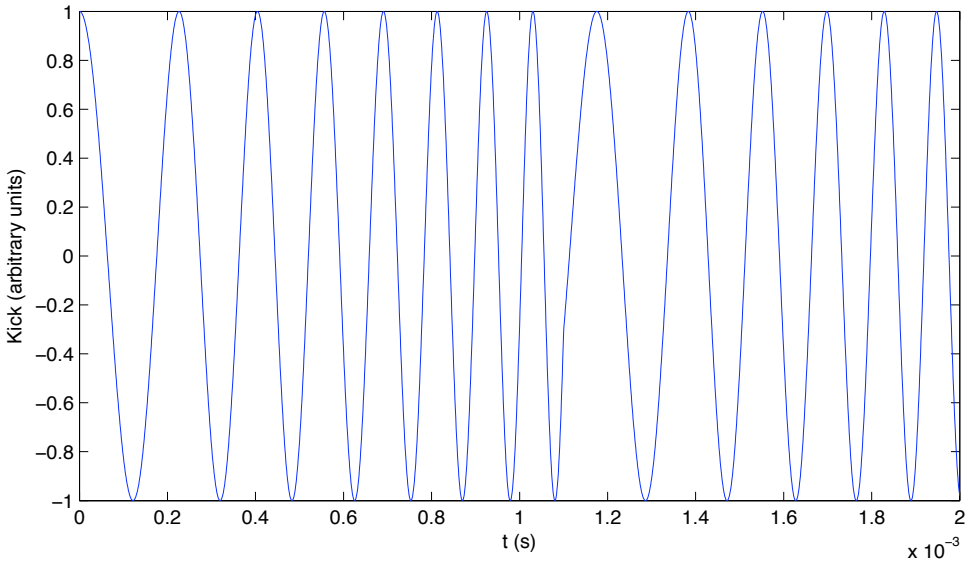

Figure 4.3: An example of a signal modulated in frequency by a saw-tooth signal. The values of the carrier wave frequency is much smaller than the frequency to be used for the kicker of the RF-knockout extraction.

4.2 Noise

A second solution to perturbate all the particles of a beam, where there is a momentum spread and the chromaticity is different from 0, involves the use of a white noise at a given range of frequency. This solution was described by S. Van der Meer in 1978 [25]. It has not been used up to now in hadrontherapy synchrotrons.

A white noise is a signal which contains the same power in each bandwidth at all the frequencies. For the RF-knockout the spectrum of the noise must contain all the range of frequencies of the particles.

The use of a white noise can eliminate the spill ripple, because the signal always contains all the frequencies of the beam.

These two solution generate an extracted beam which decays exponentially with the time [28].

To have a constant extraction the amplitude of the RF signal must increase with time.

Chapter 5

Extraction simulation

A dedicated simulation is necessary to find the better parameters for the RF-knockout extraction.

To simulate the RF-knockout extraction a multi-particle tracking program is needed.

The program has to be able to find the values of the quadrupoles and sextupoles strength to have the desired tunes and to have the desired chromaticity.

The simulation program must be able to do the tracking of at least a few thousand particles, to get an information about the extracted beam not too disturbed by the statistical fluctuations. The number of turns to be simulated is about 10^6.

The program has to change an element of the synchrotron, the kicker, at every turn.

The program *MAD-X* [29], developed at *CERN*, can find the right values of quadrupoles and sextupoles strength and it can track many particles. With *MAD-X*, the change of an element of the synchrotron during the tracking is not expected. It is possible to change all the synchrotron and to track only one turn at a time, but this procedure is very slow. I effect the *MAD-X* output is a file with all particles coordinates. Reading and writing a file for every turn is a very slow process: so *MAD-X* is not a good program to simulate the RF-knockout extraction.

For those reasons a multi-particle tracking program has been written in C++ language. The characteristics of the program are explained in next section.

5.1 Simulation program

The simulation program *ExTRACKtION* can track any number of particles (protons or carbon ions) for one turn or many turns of the synchrotron. The synchrotron lattice and the initial particle coordinates are the input of the program.

The resonance sextupole is gradually turned on in 30000 turns.

The program allows to choose whether to turn on the RF-knockout or leave it off, to choose the type of radio frequency and to select the kind of kicker to be used.

The program performs a six-dimentional tracking, where the coordinates are:

- horizontal position (X);
- horizontal divergence (PX);
- vertical position (Y);
- vertical divergence (PY);
- longitudinal position (T);
- difference from particle momentum and reference momentum, divided by the reference momentum (PT).

The synchrotron is composed by linear and nonlinear elements.

The linear elements are bending magnets, quadrupole magnets and drift spaces. These elements can be described by a transfer matrix.

$$\begin{pmatrix} X_1 \\ PX_1 \\ Y_1 \\ PY_1 \\ T_1 \\ PT_1 \end{pmatrix} = (M) \begin{pmatrix} X_0 \\ PX_0 \\ Y_0 \\ PY_0 \\ T_0 \\ PT_0 \end{pmatrix} \tag{5.1}$$

where M is the element transfer matrix, $\{X_1; PX_1; Y_1; PY_1; T_1; PT_1\}$ are the particle coordinates after the synchrotron element, $\{X_0; PX_0; Y_0; PY_0; T_0; PT_0\}$ are the particle coordinates before the synchrotron element.

M is a 6×6 matrix.

A segment of the synchrotron with only linear elements is described by the product of the transfer matrices of each element [30]. The transfer matrix is dependent on the particle momentum.

Nonlinear elements of the synchrotron are the sextupoles.

The effect of every sextupole on the particle coordinates is calculated with the thin lens approximation, described in appendix B.1. *CNAO* sextupole effective

magnetic length is 26 cm. The sextupole is considered an element with null length preceded and followed by two 13 cm drift spaces.

With the thin lens approximation, $\Delta X = 0$ and $\Delta Y = 0$.

$$\Delta X' = \frac{1}{2} l_s k' \left(X^2 - Y^2\right) \tag{5.2}$$

$$\Delta Y' = - l_s k' XY \tag{5.3}$$

where

$$k' = \frac{1}{B\rho} \left(\frac{\mathrm{d}^2 B_Y}{\mathrm{d}X^2} \right) \tag{5.4}$$

is the *normalized sextupole gradient*.

Therefore, the effect of a sextupole is:

$$X_1 = X_0 \tag{5.5}$$

$$PX_1 = PX_0 + \Delta X' \tag{5.6}$$

$$Y_1 = Y_0 \tag{5.7}$$

$$PY_1 = PY_0 + \Delta Y' \tag{5.8}$$

$$T_1 = T_0 \tag{5.9}$$

$$PT_1 = PT_0 \tag{5.10}$$

In the *CNAO* synchrotron there are two elements which can be used as kickers for the RF-knockout extraction: the horizontal tune kicker and the Schottky pickup. The elements are described in chapter 6. The simulation program consents to choose which kicker use changing an input parameter.

The kicker is considered an element with null length preceded and followed by two equal drift spaces. The effect of the kicker is only to change the horizontal divergence:

$$X_1 = X_0 \tag{5.11}$$

$$PX_1 = PX_0 + k \tag{5.12}$$

$$Y_1 = Y_0 \tag{5.13}$$

$$PY_1 = PY_0 \tag{5.14}$$

$$T_1 = T_0 \tag{5.15}$$

$$PT_1 = PT_0 \tag{5.16}$$

The normalized quadrupole gradient and the normalized sextupole gradient depend on the particle momentum. The beam has a momentum spread, therefore the normalized gradients depend on the particle.

The program generates the transfer matrix of each segment of the synchrotron composed of only linear elements for one particle, tracks the particle for all the turns or until the extraction and continues with the next particle. For each particle the matrices must be recalculated, because the particle momenta are different. The particle energy does not change during the simulation, because there is no accelerating cavity and the particles do not radiate.

The program verifies the particle horizontal coordinate at the electrostatic extraction septum. If the particle position is over the septum, the particle is considered extracted and its coordinates are stored in a file.

5.1.1 RF-Signal

The frequency modulated signal is generated according to what explained in chapter 4.

The noise signal is produced starting with the pseudo-random number generator, included in the C++ standard library: the function `rand()`.

The C++ function `rand()` returns a pseudo-random natural number in the range 0 to `RAND_MAX`. `RAND_MAX` is a constant defined in the `<cstdlib>` C++ library.

With a simple code, a signal ranging from -1 to 1 and with a flat spectrum between $f = 0$ and $f = f_s/2$, where f_s is the sampling frequency, can be obtained. A signal like that is shown in figure 5.1.

A signal with a spectrum characterized by two peaks near an angular frequency ω_0 can be obtained by means of an amplitude modulation of a sinusoid of angular frequency ω_0 with a sinusoid of angular frequency $\delta\omega$ (*Werner formulas*, eq. 5.17).

$$\cos(\delta\omega t)\cos(\omega_0 t) = \frac{1}{2}\left[\cos\left((\omega_0 - \delta\omega)\,t\right) + \cos\left((\omega_0 + \delta\omega)\,t\right)\right] \tag{5.17}$$

In general, if a sinusoid with frequency f_0 is modulated in amplitude by a signal with a frequency distribution centered at 0, a signal with the same frequency distribution, but centered at f_0, is obtained.

A noise with a flat spectrum between $f_0 - \delta f$ and $f_0 + \delta f$ in necessary for the RF-knockout extraction. To generate that signal, a signal with a flat spectrum in the range 0 to δf is used to modulate a sinusoid with a frequency f_0.

A signal with an almost flat spectrum in the range 0 to δf can be generated filtering the noise obtained with the pseudo-random generator. In the program a

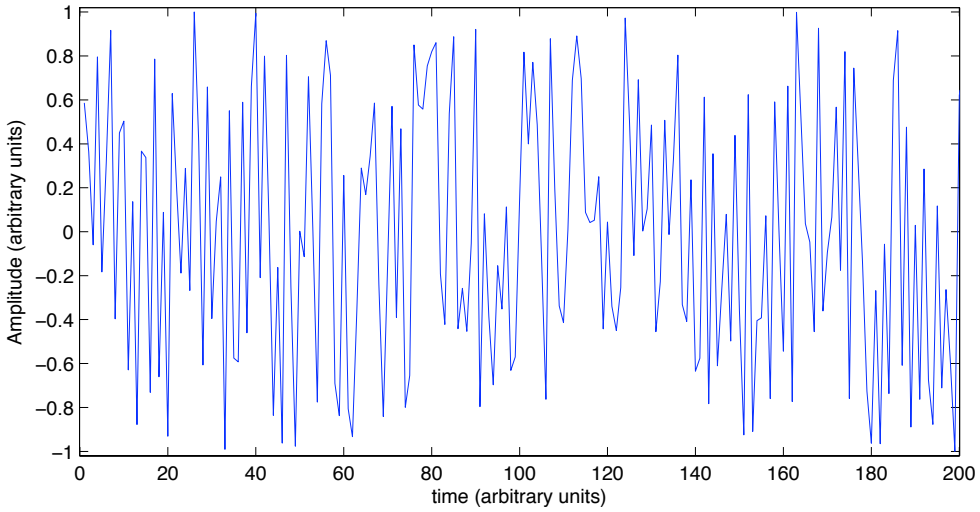

Figure 5.1: A white noise signal generated with the pseudo-random C++ generator.

gaussian filter is used.

In figure 5.2 the Fast Fourier Transform of the noise signal used for RF-knockout is shown.

5.1.2 Particle distribution

The program generates a particle distribution uniform into an ellipse, in the horizontal and vertical phase space. This distribution is similar to the *CNAO* real particle distribution in the synchrotron [31].

The horizontal and vertical emittance are free parameters.

In figure 5.3 the initial horizontal phase space distribution is shown. The emittance corresponding to this distribution is 3.66225π mm mrad, i.e. the value at the maximum extraction energy of carbon ion beam.

During the extraction the accelerating RF cavity is turned off and the momentum spread causes the beam filling all the ring after some laps.

With the carbon ion beam at maximum extraction energy and a momentum spread $\Delta p/p = 0.001$, the beam fills all the ring after about 3500 turns.

The longitudinal phase space distribution generated by the program is uniform in $\Delta p/p$, with a null value of longitudinal relative position. The initial longitudinal phase space distribution is shown in figure 5.4.

In table 5.1, the characteristics of the simulated beam are summarized.

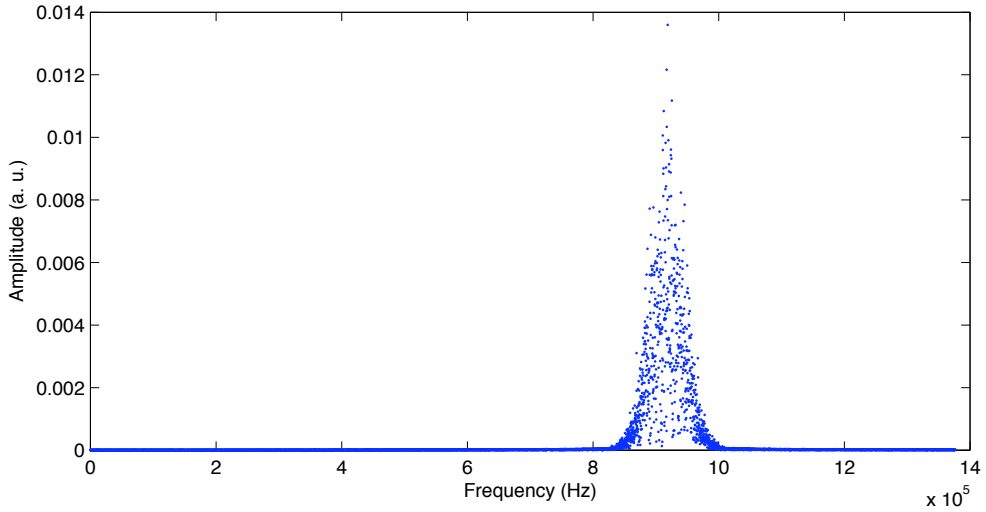

Figure 5.2: Fast Fourier Transform of the noise signal used for the RF-knockout.

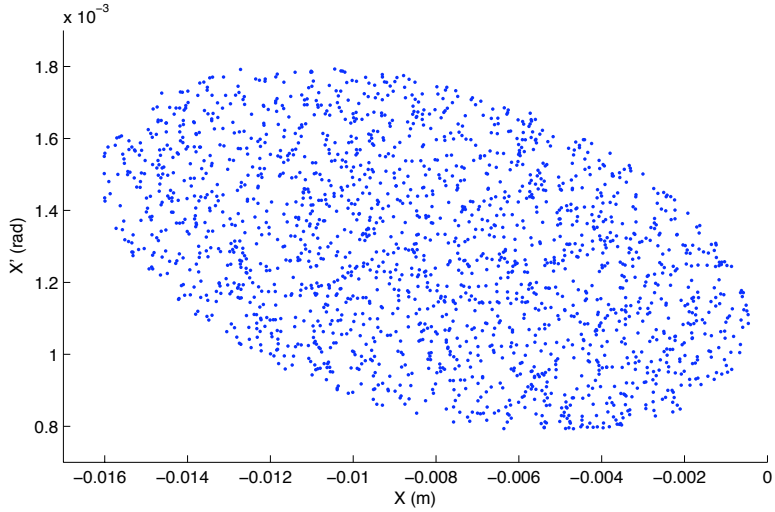

Figure 5.3: Initial horizontal phase space distribution. The emittance is 3.66225 mm mrad, the value corresponding to the maximum extraction energy of carbon ion beam.

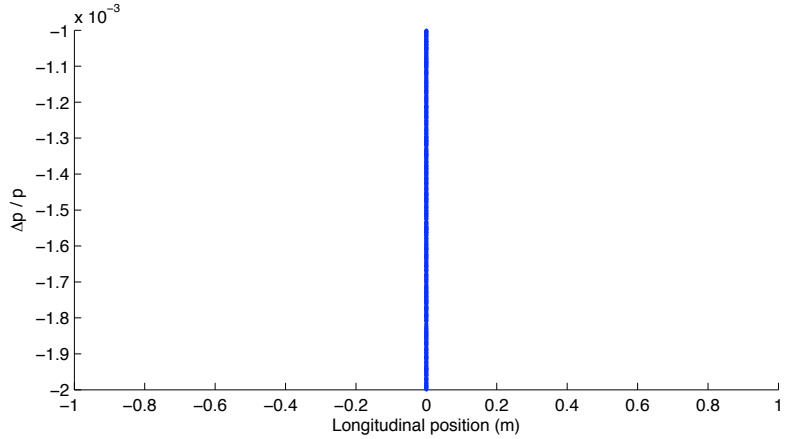

Figure 5.4: Initial longitudinal phase space distribution.

Particle	$^{12}C^{6+}$
kinetic energy	400 MeV/u
f_{Rev}	2.757 MHz
Q_x	1.666
Q_y	1.720
ξ_x	-3.940
ξ_y	-1.067
Momentum spread ($\Delta p/p$)	0.001
Momentum translation ($\delta p/p$)	-0.0015
f_{RF-ko}	0.919 MHz
ΔQ_x	0.004
ΔQ_y	0.001
$f_{Rev} \cdot \Delta Q_x$	11 kHz
$\epsilon_x = \epsilon_y$	3.66225π mm mrad

Table 5.1: Simulated beam characteristics.

5.2 Simulation results without RF-knockout

In figure 5.5 the result of the tracking of a carbon ion in the stable region without the RF-knockout is shown. The particle is tracked for 10^5 turns, the resonance sextupole is turned on in 30000 turns. In the firsts 100 turns, with the sextupole turned off, the particle horizontal phase space coordinates stay on an ellipse. After 10^5 turns, the particle coordinates stay on the triangle.

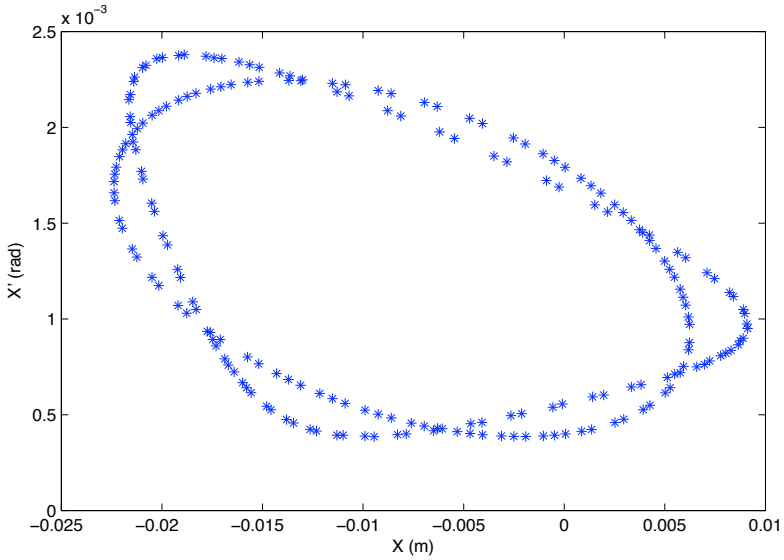

Figure 5.5: Horizontal phase space coordinates of a stable particle. Every point is the position of the particle at one turn. The points on the ellipse are the first 100 turns, with the sextupole turned off, the points on the triangle are the last 100 turns of the simulation, with the sextupole turned on.

In figure 5.6 is shown the result of the tracking of a carbon ion outside the stable region. The separatrices are visible.

To verify the dimension of the stable triangular region, 1000 particles with a large emittance have been tracked for 10^5 turns. Many particles were extracted, because they were in the unstable region. Injected particles and residual particles are shown in figure 5.7

The area of the stable region, the *acceptance* (eq. 3.23), depends on the distance of the particle tune from the resonance. The particle tunes are different, because the chromaticity is not 0 and the particles have a momentum spread.

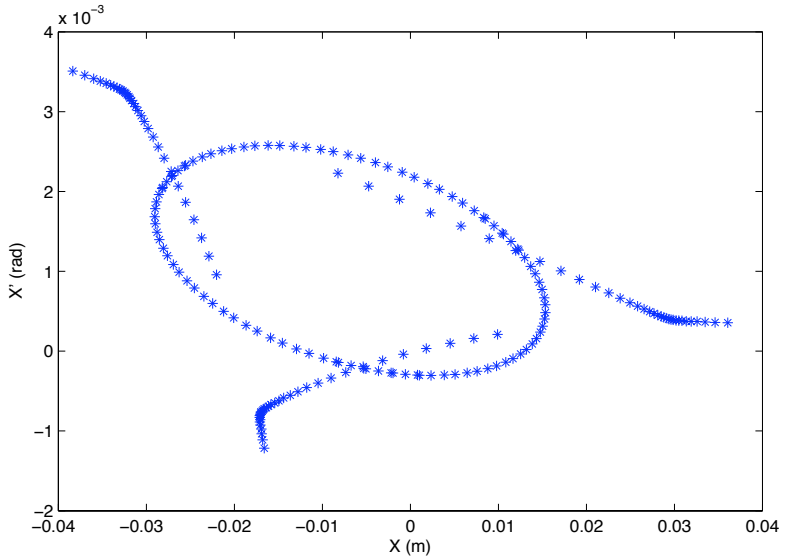

Figure 5.6: Horizontal phase space coordinates of an unstable particle. The particle is extracted after about 40000 turns.

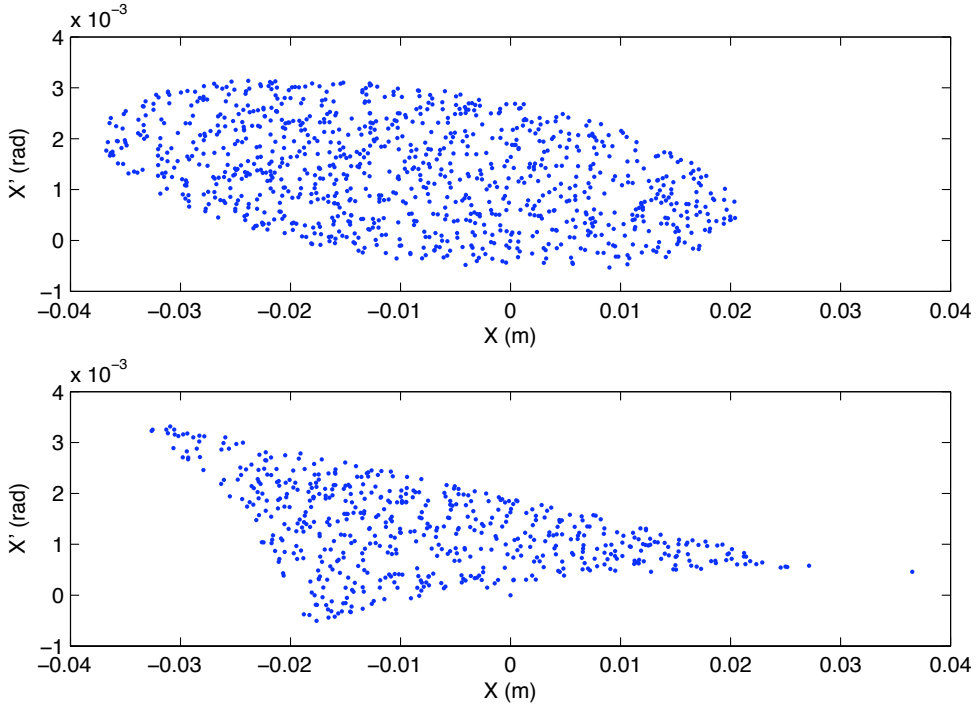

Figure 5.7: Horizontal phase space coordinates of 1000 particles without momentum spread at injection, with a large emittance, and the residual particles after 10^5 turns.

In figure 5.8 two stable regions are shown: the yellow one is relative to particles far from resonance, the blue one is relative to particles near the resonance. One of the three separatrices, the one where the extraction occurs, is common for particles with high momentum and particles with low momentum, because the lattice satisfies the *Hardt Condition*.

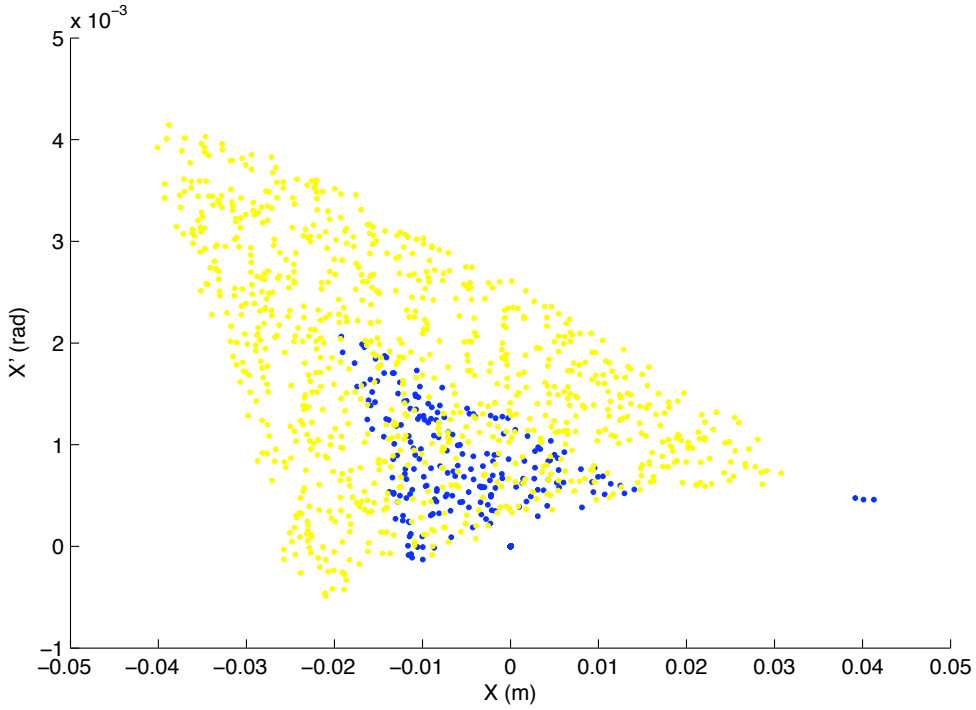

Figure 5.8: The stable regions for two groups of particles with different momenta, i.e. with different tune distance from the resonance.

5.3 Simulation with RF-knockout

To find the correct frequency of the carrier wave to be sent to the kicker, a simulation with a large FM period and a large FM amplitude was done. The amplitude of the carrier wave is large enough to have a high intensity spill.

The parameters of the RF signal used are:

$$f_k = (1 - q - \delta Q) * frev = 0.901\,\text{MHz} \tag{5.18}$$

$$Kick = 3.0\,\mu\text{rad} \tag{5.19}$$

$$\Delta f_k = 50\,\text{kHz} \tag{5.20}$$

$$TFM = 10\,\text{ms} \tag{5.21}$$

where f_k is the carrier wave frequency, $Kick$ is the amplitude of the carrier wave, Δf_k is the amplitude of the frequency modulating signal, TFM is the repetition period of the frequency modulating signal.

In figure 5.9 is shown the intensity of the extracted beam relating to the phase of the frequency modulating function.

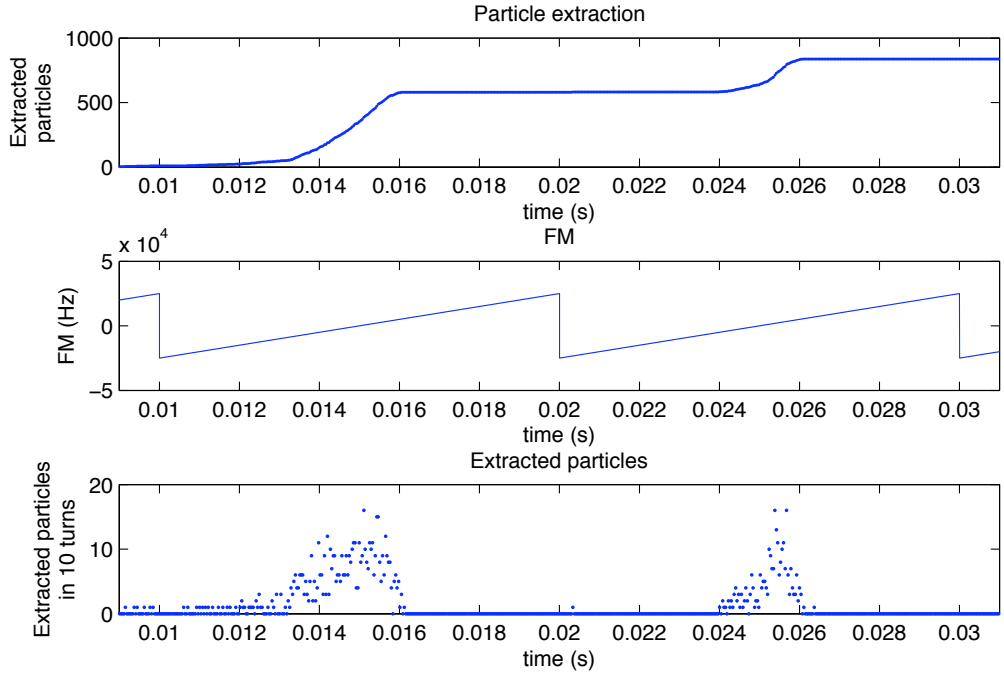

Figure 5.9: The first picture shows the integral of the extracted particles, the second one shows the frequency modulating function, the third one shows the extracted particles in 10 turns.

Extraction takes place only at a certain range of modulating function, i.e. when the instantaneous frequency of the signal matches to the betatron frequency of some particles of the beam.

If the momentum spread is null, the extracted beam intensity decay exponentially, because the beam emittance increase exponentially.

In figure 5.10 the extracted beam intensity is shown with three different constant amplitude of RF-knockout: 0.5 μrad, 1.0 μrad and 2.0 μrad. The extracted beam intensity increase at the begin of the RF-knockout and then decrease exponentially. The characteristic time of the exponential is smaller when the kick amplitude is larger.

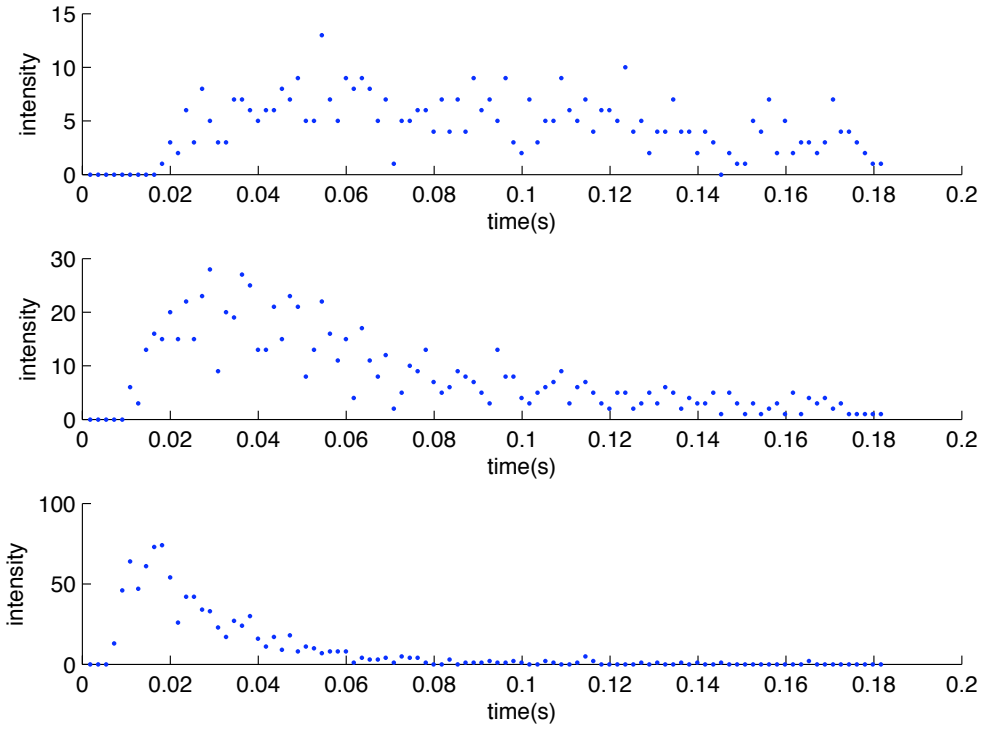

Figure 5.10: Intensity of extracted beam with constant kick amplitude: 0.5 μrad, 1.0 μrad and 2.0 μrad.

In figure 5.11 the extraction intensity is shown for beams with three different momenta, without momentum spread. The momentum variations, compared to the value of the reference momentum, are: $\delta p/p = -0.001$, $\delta p/p = -0.0015$ and $\delta p/p = -0.002$.

The intensity of the extracted beam decrease exponentially. The characteristics time of the exponential is smaller when the momentum of the particles is close to the reference momentum, i.e. the tune is close to the resonance tune and the acceptance of the stable region is smaller.

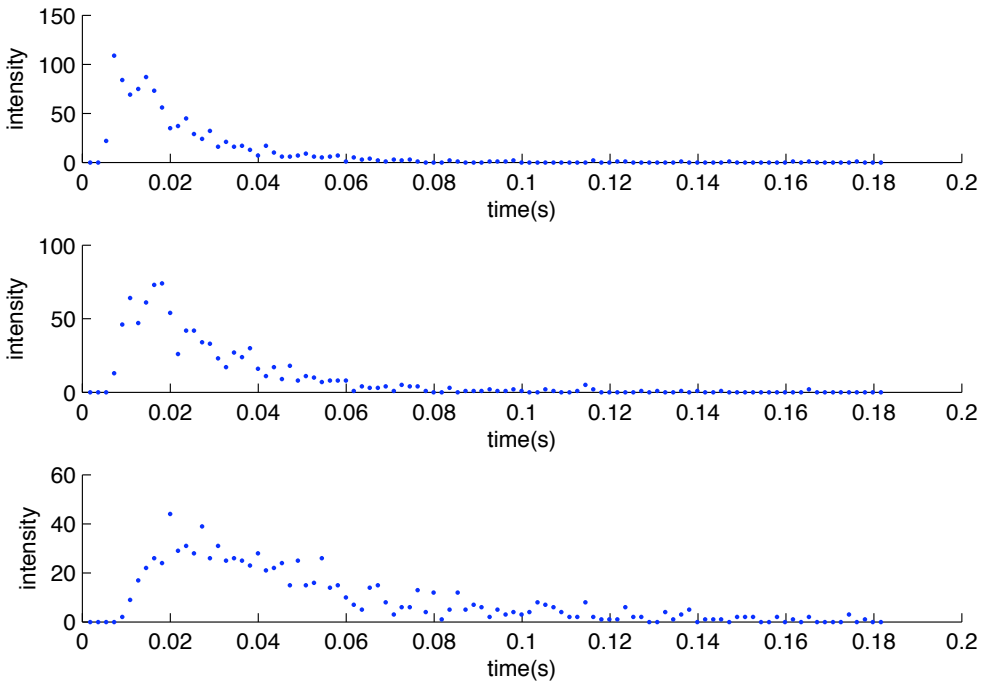

Figure 5.11: Intensity of extracted beam with constant kick amplitude, no momentum spread and three different momenta: $\delta p/p = -0.001$, $\delta p/p = -0.0015$ and $\delta p/p = -0.002$.

The frequency modulated signal for the RF-knockout covers all frequencies of the beam, but the extracted beam has a ripple corresponding to the frequency of the modulating function.

In figure 5.12, the integral of extraction current is shown together with the saw-tooth frequency modulation signal for a short time. The 1 kHz ripple is visible.

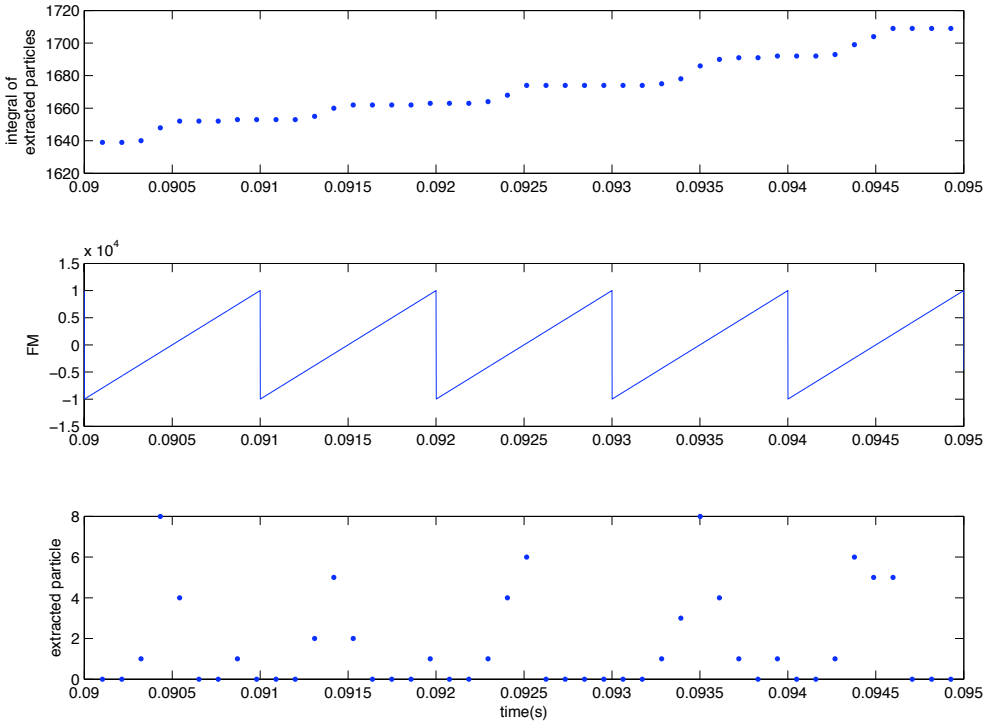

Figure 5.12: Integral of the spill; saw-tooth FM; spill with 1 kHz ripple.

Although the RF-knockout with the white noise signal is not used in the main synchrotrons for hadrontherapy, the simulation shows that the ripple is eliminated from the spill with that method. Figure 5.13 shows the spill characteristics for this case.

5.3.1 Constant spill

The extracted beam with the RF-knockout decays exponentially with time with both signals: the frequency modulated sinusoid and the white noise. The characteristic time of the exponential depends on the kick amplitude.

To have a constant spill, as it is needed for hadrontherapy, the amplitude of the signal must be increased.

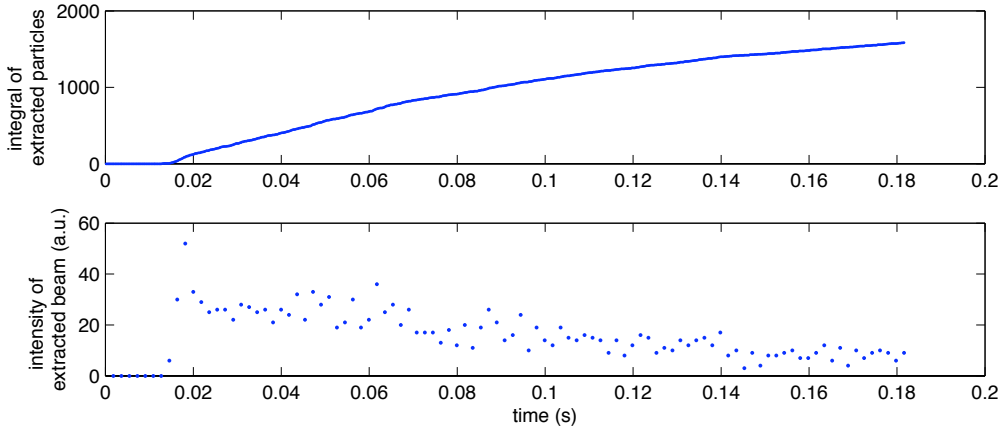

Figure 5.13: Integral of the extracted beam and spill for the RF-knockout with noise signal simulation.

In figure 5.14, the inverse of the characteristic time ($\lambda = 1/\tau$) is plotted as a function of the kick amplitude.

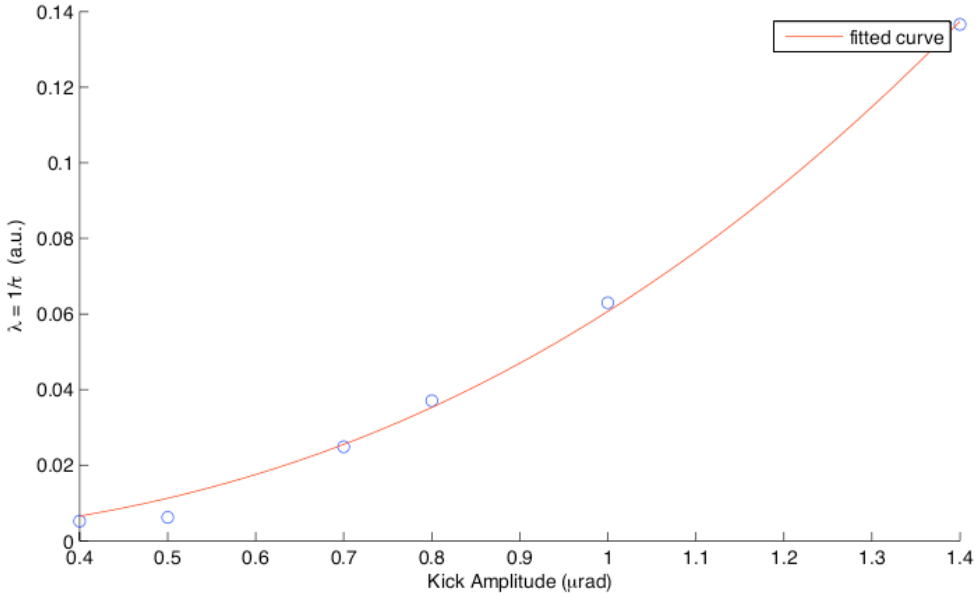

Figure 5.14: $1/\tau$ as function of kick amplitude.

A fit with a power function $\lambda = A \times k^B$ has been performed, in order to find the best approximation. It is an empirical way to estimate the value of $1/\tau$ as function of the kick amplitude.

The fit result is:

$$B = 2.4 \pm 0.1 \tag{5.22}$$

The extracted beam has an exponential decay:

$$\mathcal{N}(t) = \mathcal{N}_0\, e^{-\frac{t}{\tau}} \tag{5.23}$$

where $\mathcal{N}(t)$ is the number of particles of the beam at time t, $\mathcal{N}_0$ is the initial number of particles.

$$-\frac{\mathrm{d}\mathcal{N}(t)}{\mathrm{d}t} = \frac{\mathcal{N}(t)}{\tau} = \mathcal{N}(t) \times \lambda \tag{5.24}$$

The amplitude of the kick must be increased to have a constant spill.

$$-\frac{\mathrm{d}\mathcal{N}(t)}{\mathrm{d}t} \propto \mathcal{N}(t) \times k(t)^B = const = \mathcal{N}_0 \times k_0^B \tag{5.25}$$

$$\mathcal{N}(t) \times k(t)^B = \mathcal{N}_0 \times k_0^B \tag{5.26}$$

$$k(t) = k_0 \times (\mathcal{N}_0/\mathcal{N}(t))^{1/B} \tag{5.27}$$

where $\mathcal{N}(t) = \mathcal{N}_0 \times (1 - t/\tau)$.

In figure 5.15, the kicker signal has been increased with the amplitude modulation function of equation 5.27.

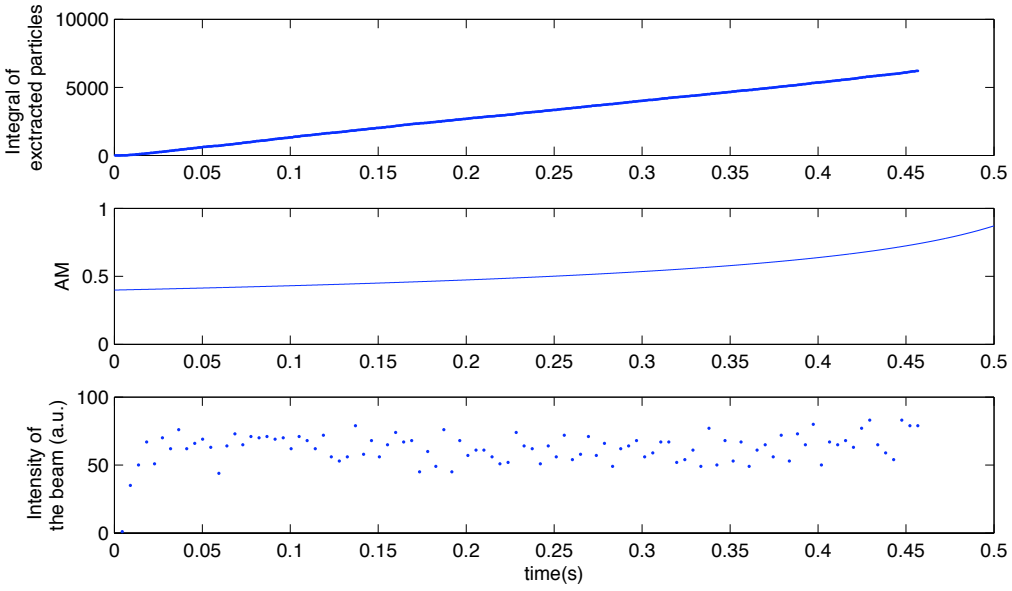

Figure 5.15: Spill integral, AM, spill.

Spill integrals of 0.1 s long periods in different moments have been compared and they differ by about 10% for the first 70% of the extraction.

A feedback system could be useful to have a constant extraction of the last part of the beam.

The horizontal distribution of the particles in six moments of the simulation is shown in figure 5.16.

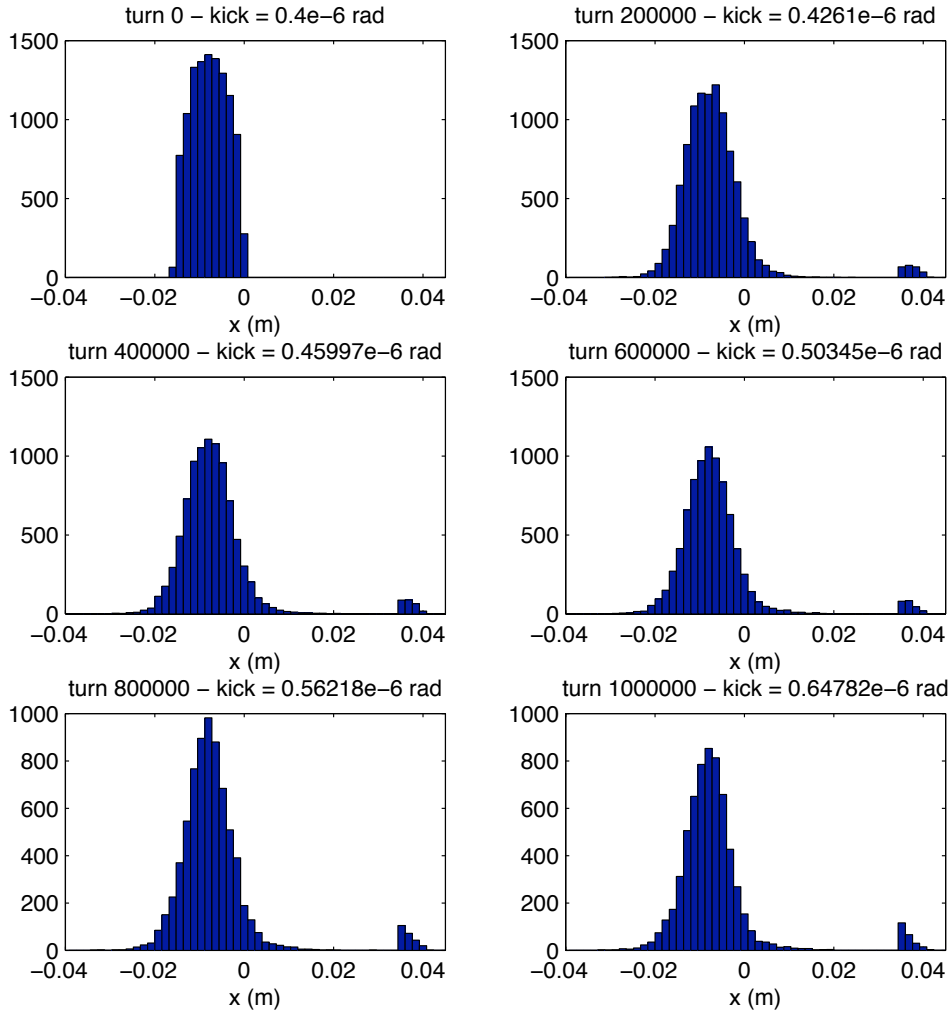

Figure 5.16: Horizontal distribution of the beam at six different moments of the simulation. The peak at $x = 0.035\,\mathrm{m}$ is the extracted beam.

In figure 5.17, the horizontal phase space distribution of the extracted beam is shown. The RMS emittance of the extracted beam obtained from the simulation is $\epsilon_{RMS} = 2.358 \cdot 10^{-2}\,\text{mm mrad}$.

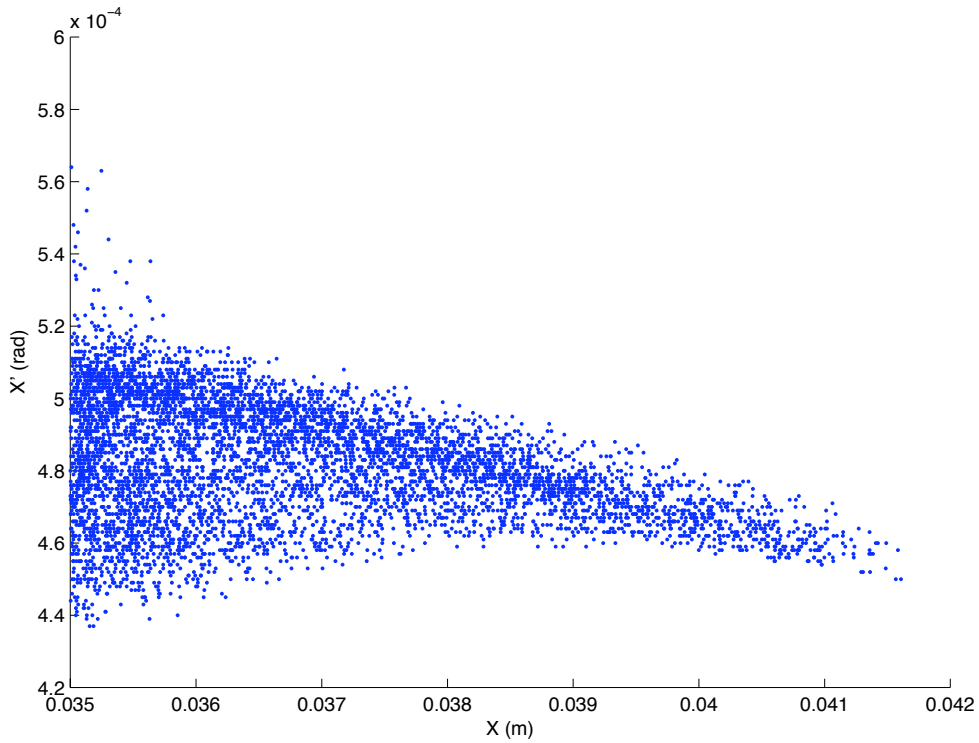

Figure 5.17: Horizontal phase space distribution of the extracted beam.

5.4 Simulation: a conclusion

Two signals have been compared for the RF-knockout extraction: a frequency modulated sinusoid signal and a white noise filtered with a gaussian filter. With the frequency modulated signal, the extracted beam has a ripple at the frequency of the modulating signal (1 kHz). The noise signal does not produce an extracted beam with ripple, so it is preferable.

An extracted beam with constant intensity is possible by means of an amplitude modulation of the kicker signal. The simulation has shown an amplitude modulation function which produce an extracted beam with constant intensity for about first 70% of the extraction time. A feedback system could be useful to have a constant spill in the last part of the extraction.

The simulation has shown that, in the most demanding conditions, i.e. with

a carbon ion beam at maximum energy and minimum emittance, a relatively fast extraction (1 s) can be obtained with a perturbation of less than 1 μrad. To have a slower extraction, an extraction of the proton beam or an extraction of the carbon ion beam at less energy, the perturbation should be smaller.

Chapter 6

Kicker

The maximum needed amplitude of the kick, as shown by simulation, is about 1 μrad. Two devices could be used for the RF-knockout extraction in CNAO synchrotron: the horizontal tune kicker [20] or the Schottky pickup [32].

The horizontal tune kicker is a dipole used to transversally perturb the beam, so to measure the horizontal tune. In figure 6.1 the horizontal tune kicker is shown.

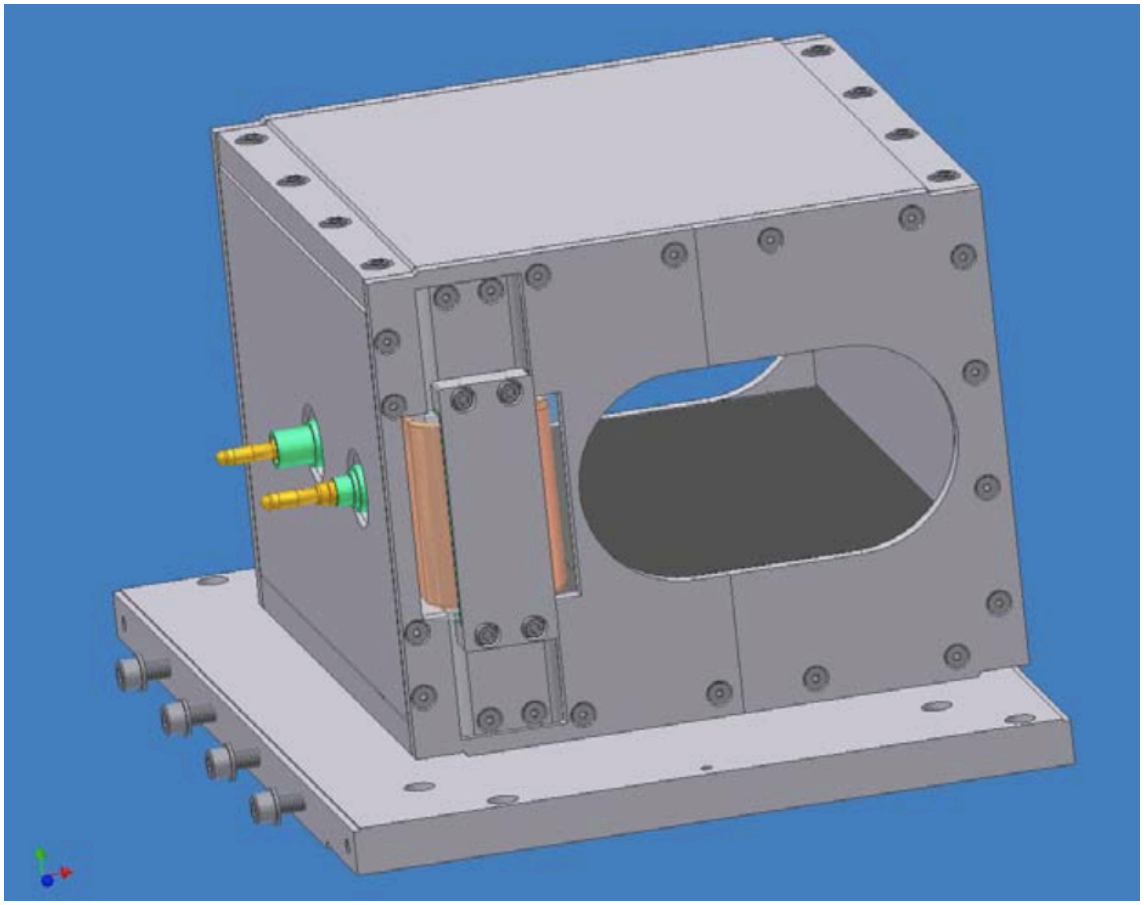

Figure 6.1: Horizontal tune kicker.

The deflection angle of particles passing through the kicker per unit of coil current is $\Delta x' \simeq 0.7\,\mu\text{rad/A}$ [33].

The resistance of the tune kicker is $R = 4.3{\cdot}10^{-3}\,\Omega$, the inductance is $L = 0.7\,\mu\text{H}$. At 1 MHz, the reactance $L\omega$ is of the order of $2\pi\,\Omega$, which is much larger than the resistance.

With a current flowing through the magnet of 10 A, corresponding to a deflection of $7\,\mu$rad, the voltage across the kicker will be:

$$V = ZI \simeq jL\omega I \simeq 100\,\text{V} \tag{6.1}$$

A power supply with these characteristics is commercially available, so the horizontal tune kicker can be used for the RF-knockout extraction.

The Schottky pickup is a diagnostic element of the synchrotron made by stripline electrodes, used to measure the longitudinal and transverse dynamical properties of the circulating beam. It can be relatively easily turned in a beam kicker. In figure 6.2 the schottky pickup is shown.

The electric field generated in the Schottky pickup, with a voltage applied to the electrodes of $\pm 500\,\text{V}$, is $10^4\,\text{V/m}$ [33]. The deflection angle can be calculated for the carbon ion beam at maximum energy:

$$\Delta x' = \frac{E \cdot q \cdot l}{p \cdot \beta c} \simeq \frac{10^4\,\text{V/m} \cdot 6\,\text{e} \cdot 1\,\text{m}}{11.4\,\text{GeV/c} \cdot 0.71\,\text{c}} \simeq 7.4\,\mu\text{rad} \tag{6.2}$$

where E is the electric field, q is the particle charge, l is the electrode length, p is the particle momentum and $\beta = v/c$. This is the deflection due to the electric field. The total deflection is greater, because a component due to the magnetic field, produced by current flowing in the electrodes, must be added.

The necessary kick for the RF-knockout extraction is less than $1\,\mu rad$, so the Schottky pickup can be used.

These two devices are in different regions of the ring. The simulation has not shown relevant differences between the two kicker positions.

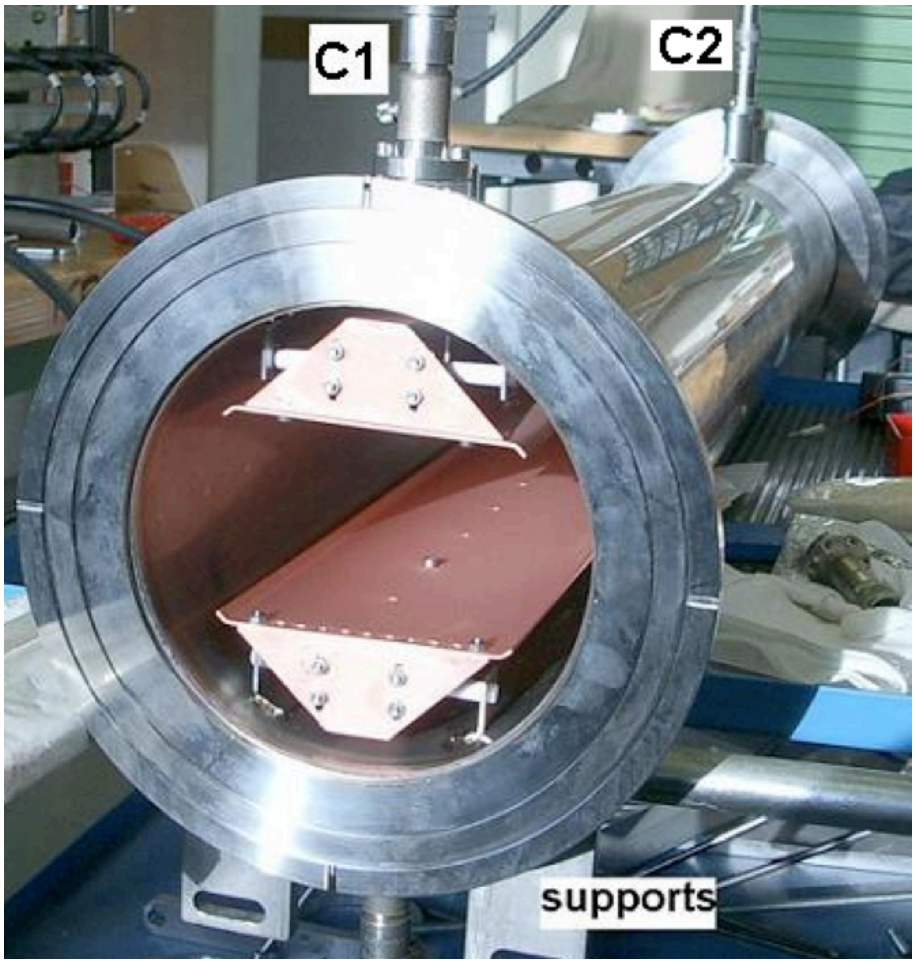

Figure 6.2: Schottky pickup.

Conclusions

CNAO accelerator complex is now under commissioning. The commissioning of the injection system is successfully concluded. Design beam parameters have been obtained along the injector, including the two sources, the *LEBT*, the *RFQ*, the *LINAC* and the *MEBT*.

A slow extraction system from the synchrotron with high precision intensity is needed. Two extraction methods will be possible in the *CNAO* synchrotron: the acceleration driven extraction, with the use of a betatron core, and the RF-knockout.

After analysis and evaluations, the feasibility of the RF-knockout extraction in the *CNAO* synchrotron has been checked.

The program *ExTRACKtION* has been written and used to fully explore the possibility of implementing the RF-knockout extraction method in the *CNAO* synchrotron with the existing hardware. It will be also used to simulate the beam dynamics with any extraction systems and to obtain the beam distribution on the extraction line in order to optimize the extracted beam characteristics.

In this work the use of a filtered white noise, instead of a frequency modulated sinusoid, as kicker signal has been proposed to eliminate the ripple of the RF-knockout extracted beam.

The maximum kick amplitude needed to have a slow and uniform extraction can be produced by two devices already present in the *CNAO* synchrotron: the horizontal tune kicker and the Schottky Pickup.

When the commissioning of the synchrotron will be terminated, the RF-knockout extraction will be tested on the synchrotron.

Appendix A

Accelerator Physics

A.1 Coordinate system

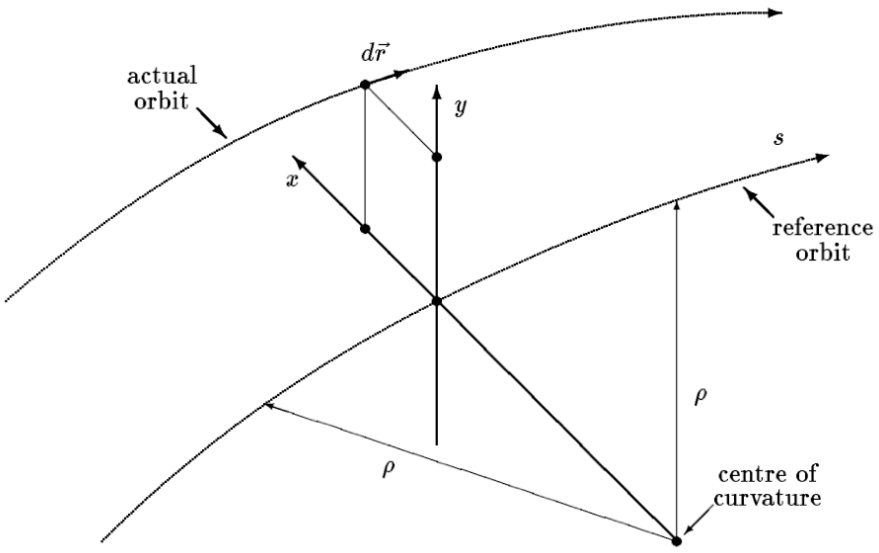

Figure A.1: Coordinate system for particle accelerator physics.

In particle Accelerator Physics an accelerator is described as a sequence of elements placed along the reference orbit. The reference orbit is the orbit of an ideal particle with the exact momentum. It is defined under the assumption that all elements are perfectly aligned.

The position of a particle in the accelerator is defined by the curvilinear coordinate s, along the reference orbit, and by the orthogonal coordinates x and y. The x axis is on the plane of the accelerator and the positive direction is going outside the synchrotron. The y axis is the vertical coordinate.

A.2 Emittance and acceptance

The beam emittance is the region of phase space occupied by the particles of the beam. There are the horizontal, vertical and longitudinal emittance. The unit of measure is m $\times$ rad. Usually the emittance is expressed in mm $\times$ mrad.

The acceptance is the maximum area which the beam can occupy in phase space without losing particles.

Appendix B

Third order resonance

B.1 Effect of a sextupole on the beam

The magnetic field of a sextupole is:

$$B_x = \left(\frac{\mathrm{d}^2 B_y}{\mathrm{d}x^2}\right) xy \qquad\qquad B_y = \frac{1}{2}\left(\frac{\mathrm{d}^2 B_y}{\mathrm{d}x^2}\right)\left(x^2 - y^2\right) \tag{B.1}$$

$$G = \frac{\mathrm{d}^2 B_y}{\mathrm{d}x^2} \tag{B.2}$$

is the sextupole gradient.

The effect of a sextupole magnet on the trajectory of a positively charged particle in an anticlockwise synchrotron can be calculated with the thin lens approximation. The sextupole will produce a Δp_x and therefore a $\Delta x'$ according to:

$$\Delta p_x = \int F_x \mathrm{d}t = q B_y l_s \tag{B.3}$$

where l_s is the length of the sextupole and q is the charge of the particle;

$$\Delta x' = \frac{\Delta p_x}{p} = \frac{q B_y l_s}{p} \tag{B.4}$$

In eq. B.4, substituting $\frac{p}{q}$ with $B\rho$ (eq. 2.2):

$$\Delta x' = \frac{B_y l_s}{B\rho} \tag{B.5}$$

Similarly for y' correction:

$$\Delta y' = -\frac{B_x l_s}{B\rho} \tag{B.6}$$

The values B_x and B_y from eq. B.1 are substituted into eq. B.5 and eq. B.6:

$$\Delta x' = \frac{1}{2} l_s k' \left(x^2 - y^2\right) \tag{B.7}$$

$$\Delta y' = -\, l_s k'\, xy \tag{B.8}$$

where

$$k' = \frac{1}{B\rho} \left(\frac{\mathrm{d}^2 B_y}{\mathrm{d}x^2}\right) \tag{B.9}$$

is the *normalized sextupole gradient*.

Now the transformations for normalized coordinates are applied to the equations B.7 and B.8, in order to obtain the effect of a sextupole in normalized coordinates.

Normalized coordinates are defined as [30]:

$$X = \frac{x}{\sqrt{\beta_x}} \tag{B.10}$$

$$X' = \sqrt{\beta_x}\, x' \tag{B.11}$$

$$Y = \frac{y}{\sqrt{\beta_y}} \tag{B.12}$$

$$Y' = \sqrt{\beta_y}\, y' \tag{B.13}$$

Therefore the effect of a sextupole in normalized coordinates results to be:

$$\Delta X = 0 \tag{B.14}$$

$$\Delta X' = \left(\frac{1}{2}\, {\beta_x}^{\frac{3}{2}} l_s k'\right) \left(X^2 - \frac{\beta_y}{\beta_x} Y^2\right) = S \left(X^2 - \frac{\beta_y}{\beta_x} Y^2\right) \tag{B.15}$$

$$\Delta Y = 0 \tag{B.16}$$

$$\Delta Y' = -2 \left(\frac{1}{2}\, {\beta_x}^{\frac{3}{2}} l_s k'\right) \frac{\beta_y}{\beta_x} XY = -2\, S\, \frac{\beta_y}{\beta_x} XY \tag{B.17}$$

where

$$S = \left(\frac{1}{2}\, {\beta_x}^{\frac{3}{2}} l_s k'\right) \tag{B.18}$$

is the *normalized sextupole strength*.

The sextupoles cause the coupling between X and Y.

In the case of the resonant extraction, the amplitude of the horizontal coordinate is much greater than the amplitude of the vertical coordinate, furthermore, the tune of the vertical betatron oscillations has a value far from resonances. For these reasons, the vertical coordinate is negligible in the study of the resonant extraction

and equations B.14, B.16, B.15, B.17 get this simplified form:

$$\Delta X = 0 \tag{B.19}$$

$$\Delta X' = S\,X^2 \tag{B.20}$$

$$\Delta Y = 0 \tag{B.21}$$

$$\Delta Y' = 0 \tag{B.22}$$

Bibliography

[1] G. Bazzano. Status of the commissioning of the centro nazionale di adroterapia oncologica (CNAO). *Proceedings of IPAC10*, 2010.

[2] N. Carmignani, C. Biscari, M. Serio, G Balbinot, J. Bosser, E. Bressi, M. Caldara, M. Pullia, and G. Venchi. RF-Knockout extraction system for the CNAO Synchrotron. *Proceedings of IPAC10*, 2010.

[3] C. Amsler et al. The Review of Particle Physics. *Physics Letters*, B(667), 2008.

[4] Hirohiko Tsujii. Overview of carbon ion radiotherapy at nirs. *Proceedings of II NIRS-CNAO Joint Symposium on Hadrontherapy*, 2010.

[5] S. Yamada et al. Carbon ion therapy for patients with locally recurrent rectal cancer. *Proceedings of II NIRS-CNAO Joint Symposium on Hadrontherapy*, 2010.

[6] Hirohiko Tsujii. Carbon ion radiotherapy for prostate cancer. *Proceedings of II NIRS-CNAO Joint Symposium on Hadrontherapy*, 2010.

[7] U. Amaldi. The Italian hadrontherapy project CNAO. *Physica Medica*, Vol. XVII, 2001.

[8] L. Badano et al. Proton-ion medical machine study (PIMMS). *CERN/PS 99-010 (DI)*, Part 2, 1999.

[9] G. Ciavola, L. Gammino, Maimone F., A. Galatà, M. Pullia, R. Monferrato, C. Bieth, W. Bougy, G. Gaubert, O. Tasset, and A. C. C. Villari. Commissioning of the ECR ion sources at CNAO facility. *Proceedings of EPAC08*, 2008.

[10] Fondazione Tera. Ion Sources for CNA project. *TECHNICAL NOTE (TN)*, 2003.

[11] B. Schlitt, G. Clemente, C. M. Kleffner, M. Maier, A. Reiter, W. Vinzenz, H. Vormann, E. Bressi, M. Pullia, E. Vacchieri, S. Vitulli, C. Biscari, A. Pisent, P. A. Posecco, and C. Roncolato. Linac commissioning at the Italian Hadrontherapy Centre CNAO. *Proceedings of IPAC10*, (MOPEA003), 2010.

[12] J. Bosser, G Balbinot, S. Bini, M. Caldara, V. Chimenti, L. Lanzavecchia, A. Parravicini, A. Clozza, and V. Lollo. A compact and versatile diagnostic tool for CNAO injection line. *Proceedings of EPAC08*, 2008.

[13] E. Bressi, M. Pullia, and C. Biscari. Status report on the centro nazionale di adroterapia oncologica (CNAO). *Proceedings of PAC09*, 2009.

[14] G. Borri. Main quadrupole of the CNAO synchrotron (based on the PIMM study). *PS/DI/Note*, 1999.

[15] S. Rossi. The sextupole of the CNAO synchrotron (based on the PIMM study). *PS/DI/Note*, 1999.

[16] M. Crescenti, A. Susini, G. Primadei, F. J. Etzkorn, A. Schnase, and C. Fougeron. The vitrovac cavity for the tera/pimms medical synchrotron. *Proceedings of EPAC2000*, 2000.

[17] G. Franzini, D. Pellegrini, M. Serio, A. Stella, M. Donetti, M. Pezzetta, and M. Pullia. Measurements on an A/D interface used in the power supply control system of the main dipoles of CNAO. *Proceedings of EPAC08*, 2008.

[18] S. Rossi. Developments in proton and light-ion therapy. *Proceedings of EPAC06*, 2006.

[19] Iker Rodríguez García. *Calculation methodology and fabrication procedures for Particle Accelerator strip-line kickers: application to the CTF3 combiner ring extraction kicker and TL2 tail clippers.* PhD thesis, Universidad Politécnica de Madrid, 2009.

[20] J. Borburgh, M. Crescenti, A. Fower, M. Hourican, K. Metzmacher, and L. Sermeus. Final design, special magnets. *CNAO Technical note CNA-TNDP-006WXX-00231*, 2003.

[21] L. Badano et al. Proton-ion medical machine study (PIMMS). *CERN/PS 99-010 (DI)*, Part 1, 1999.

[22] M. Pullia. Transverse aspects of the slowly extracted beam. *CERN/PS 2000-06 (DR)*, 2000.

[23] L. Badano and S. Rossi. Characteristics of a Betatron Core for extraction in a proton-ion medical synchrotron. *PS/DI/Note*, 1997.

[24] K. Noda, T. Furukawa, S. Shibuya, M. Muramatsu, T. Uesugi, M. Kanazawa, M. Torikoshi, E. Takada, and S. Yamada. Source of spill ripple in the RF-KO slow-extraction method with FM and AM. *Nuclear Instruments and Methods in Physics Research A*, July 2002.

[25] S. Van der Meer. Stochastic extraction, a low-ripple version of resonant extraction. *CERN/PS/AA 78-6*, 1978.

[26] D7 - review of extraction systems (wp 3.1). 2008.

[27] Stéphane Mallat. *A wavelet tour of signal processing.* Elsevier, third edition, 2009.

[28] T. Furukawa, K. Noda, M. Muramatsu, T. Uesugi, S. Shibuya, H. Kawai, E. Takada, and S. Yamada. Global spill control in RF-knockout slow-extraction. *Nuclear Instruments and Methods in Physics Research*, A 522, 2004.

[29] MAD-X Home Page. `http://mad.web.cern.ch/mad/`.

[30] Helmut Wiedemann. *Particle Accelerator Physics.* Springer, third edition, 2007.

[31] M. Pullia. Private comunication.

[32] M. Caldara and A. Parravicini. Schottky pickups: assembling and electrical tests. *CNAO Technical note CNA-TNDF-011WXX-03821*, 2004.

[33] J. Bosser. Private comunication.